

Energy tunnels as an opportunity for sustainable development of urban areas

*Original*

Energy tunnels as an opportunity for sustainable development of urban areas / Barla, M., Insana, A.. - In: TUNNELLING AND UNDERGROUND SPACE TECHNOLOGY. - ISSN 0886-7798. - ELETTRONICO. - 132:(2023).  
[10.1016/j.tust.2022.104902]

*Availability:*

This version is available at: 11583/2974034 since: 2022-12-21T17:54:48Z

*Publisher:*

Elsevier

*Published*

DOI:10.1016/j.tust.2022.104902

*Terms of use:*

This article is made available under terms and conditions as specified in the corresponding bibliographic description in the repository

*Publisher copyright*

Elsevier postprint/Author's Accepted Manuscript

© 2023. This manuscript version is made available under the CC-BY-NC-ND 4.0 license  
<http://creativecommons.org/licenses/by-nc-nd/4.0/>. The final authenticated version is available online at:  
<http://dx.doi.org/10.1016/j.tust.2022.104902>

(Article begins on next page)

# 1 **Energy tunnels as an opportunity for sustainable development of urban areas**

2 Marco Barla, Alessandra Insana

3 Dept. of Structural, Geotechnical and Building Engineering, Politecnico di Torino, Italy

4

5

6

## 7 **ABSTRACT**

8 The use of renewable energies will be increasingly necessary to reduce carbon dioxide emissions. An important  
9 contribution can be provided by energy tunnels, which make it possible to draw on a form of clean, renewable  
10 and locally accessible thermal energy for heating and air conditioning of buildings. The paper describes the  
11 characteristics of an energy tunnel and the design aspects necessary for its conception. Explicit reference will  
12 be made to the studies conducted at the Politecnico di Torino which led to the development of an innovative  
13 energy segment which was then used to create an experimental prototype in the true size of an energy tunnel.  
14 The data collected allowed to evaluate the performance of the system and to study the possibility of thermally  
15 activating the tunnels of the future Line 2 of the Turin Metro, allocating the heat partly to the air conditioning  
16 of the stations and partly to external users. With a view to sustainable urban development, the possibility of  
17 integration with district heating systems and the possible creation of local heat distribution networks at  
18 different temperatures, directly connected to the underground infrastructure, is particularly attractive and  
19 promising.

20

## 21 **1 INTRODUCTION**

22 The growing energy demand has been increasingly leading to the spread of renewable sources-based systems.  
23 In the next years, it will be crucial to enhance the use of such systems, especially in urban areas, to cut down  
24 on carbon dioxide emissions and to meet the goals agreed in the European context (Directive, 2009; European  
25 Commission 2016).

26 Among renewable resources, low-enthalpy geothermal plants are today common practice in many countries to  
27 supply heating and cooling through a clean and locally accessible form of thermal energy (Lund et al., 2011).  
28 Shallow geothermal energy, up to 400 m depth, takes advantage of the underground as a heat tank that can be  
29 tapped into for heating in winter and where buildings' excess heat can be stored in summer. At a depth of  
30 around 8-10 m, the soil temperature is essentially stable and is marginally affected by seasonal air temperature  
31 fluctuations. In mild climates soil temperature at these depths ranges from 8 to 16°C, being generally warmer  
32 than the external air in winter and colder in summer. In these contexts, heat transfer, by means of a geothermal  
33 heat pump system, can be advantageous.

34 Beyond conventional closed-loop GSHP (Ground Source Heat Pump) systems, where heat exchange occurs  
35 between the ground and a heat carrier fluid flowing in the circuit installed in vertical or horizontal loops, or  
36 open-loop GWHP (Groundwater heat pump) systems, where heat exchange takes place with the groundwater  
37 itself through extraction and reinjection wells, today shallow geothermal energy also includes the so-called  
38 energy geostructures. The latter are geotechnical structures, e.g. deep and shallow foundations, diaphragm  
39 walls and tunnel linings that are suitably equipped to exchange heat with the ground (Brandl, 2006; Laloui and  
40 Di Donna, 2013; Barla and Di Donna, 2016).

41 Fitting reinforced concrete structural elements out with heat exchangers in lieu of traditional geothermal plants  
42 not only is particularly convenient from the economic perspective, since structural and energy needs are  
43 condensed into one single element, but it is also optimal from the physical standpoint because concrete is a  
44 material characterized by a good thermal conductivity and heat capacity.

45 Thermal activation of structural elements is done through the arrangement of a high-density polyethylene pipe  
46 closed loop where the heat carrier fluid circulates.

47 The interest in the application of this technology to tunnel linings is driven by the fact that the ground-contact  
48 surface is far greater compared to piles and base slabs. The heat exchanged by the lining with the surrounding  
49 ground can have multiple purposes, from heating and cooling of subway stations and substations (Bidarmaghz  
50 et al., 2023) or buildings near the tunnel (Nicholson et al., 2014; Barla et al., 2016) or heating the lining itself  
51 (Zhang et al., 2014), to deicing of bridge decks, rails and routes strengthening both safety and durability (Islam  
52 et al., 2006; Baralis et al. 2020).

53 After the pioneering experiences in Austria and Germany (Unterberger et al., 2004; Adam and Markiewicz,  
54 2009; Schneider and Moormann, 2010; Frodl et al., 2010; Franzius and Pralle, 2011; Moormann et al., 2016),  
55 followed by those in South Korea and China (Lee et al., 2012; Lee et al., 2016; Zhang et al., 2013; Zhang et  
56 al., 2014), in 2016, an innovative, optimized energy segment was designed at Politecnico di Torino (Barla and  
57 Di Donna, 2016b), i.e. Enertun. Next, a full-scale experimental prototype of an energy tunnel was installed in  
58 Turin Metro Line 1 South Extension. Data collected between 2017 and 2018 enabled the assessment of the  
59 technology performance in the city underground. The research with its promising outcomes was preparatory  
60 for launching the feasibility study of the future Metro Line 2 geostructures' thermal activation.

61 For the quantification of the geothermal potential achievable from the 27.6 km of the Line 2 tunnels, a  
62 methodological approach based on numerical finite-elements, thermo-hydraulic analyses was developed. The  
63 study resulted in drawing up a proposal on heat utilization which will be partially devoted to stations climate  
64 control and partially delivered to external customers. In view of sustainable urban development, the integration  
65 possibilities with district heating systems are indeed particularly attractive. Local, prospective district heating  
66 networks at different temperature levels, directly connected to the underground infrastructure could be  
67 accomplished. The project embodies the first experience ever worldwide to study the application of the

68 technology to such an extensive scale and its potential implementation would represent a noticeable  
69 technological and innovation challenge.

70 To provide a comprehensive picture, in the following the main characteristics of energy tunnel linings and  
71 their technological and design aspects will be discussed. Then, the experimental prototype built in Turin will  
72 be described together with the illustration of the methodological approach used for the application to Metro  
73 Line 2 and the results obtained.

74

## 75 **2 ENERGY TUNNELS**

### 76 **2.1 The concept of energy geostructures**

77 Energy geostructures are all those geotechnical-structural works such as a foundation or a diaphragm wall able  
78 to combine the twofold aim of structural stability and heat exchange with the surrounding ground in one single  
79 element (Brandl, 2006; Barla and Perino, 2014). The members of the geotechnical structure are coupled with  
80 closed systems able to absorb heat from the ground they are in contact with and to deliver it to the heat pump  
81 that will make it available to final users.

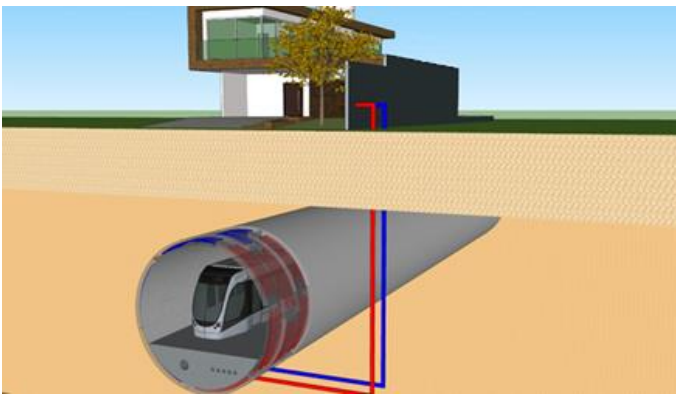
82 The main advantage of heat exchanger loops embedment lies in the reduction of geothermal plant building  
83 costs as the concrete elements are already required for structural reasons and do not need bespoke excavations  
84 or drillings. Conversely, the main drawback is the almost exclusive viability for newly constructed buildings,  
85 although some recent studies highlighted that there could be broad possibilities of application in buildings  
86 retrofitting too (Ronchi et al., 2018).

87 The use of energy geostructures began in the 80s, with the first examples related to base slabs. Then, the use  
88 widened to other geostructural assets, such as piles and walls. Many case studies that can be found in literature  
89 witness the success of energy geostructures built in Austria, Germany, UK, Switzerland (Brandl, 2006; Adam  
90 and Markiewicz, 2009; Preene and Powrie, 2009; Barla and Di Donna, 2016; Di Donna et al., 2016; Di Donna  
91 et al., 2017; Bourne Webb and da Costa Goncalves, 2016; Bourne Webb et al., 2016; Laloui and Di Donna,  
92 2013).

93 Thermal activation of tunnel linings is probably less common. Nevertheless, this application could play a  
94 relevant role in coping with the growing energy demand. As mentioned, the ground-contact exchange surface  
95 is much more extensive compared to foundations. Moreover, when resorting to mechanized tunnelling, the  
96 lining ring consists of precast segments that are mounted on-site by the TBM (Tunnel Boring Machine).  
97 Therefore, segments can be equipped with heat exchangers in the manufacturing plant itself with low extra  
98 costs and limited influence on the tunnel construction phases. The geothermal plant, once completed, can also  
99 find an application for hot tunnels cooling, where trains and cars transit might represent in some cases an  
100 additional heat source.

101 **2.2 Specific features of energy tunnels**

102 Over recent years there has been a growing interest in the energy mining of tunnel linings. Technologies  
103 harnessing the geothermal potential of water available in the rock mass are well-established, especially in  
104 Switzerland (Rybach, 1995; Wilhelm and Rybach, 2003) and, generally speaking, in alpine regions. In this  
105 case, water inflows are collected with the purpose of heating nearby buildings, as in traditional heat exchange  
106 systems. Conversely, the idea behind energy tunnels is to exchange heat with the surrounding ground through  
107 the lining. A schematic view of the operation principle is presented in Fig. 1, where the geothermal loops  
108 within the tunnel lining can displace heat from the ground to the surface and vice versa.



109  
110 Fig. 1 Schematic view of the operation principle of energy tunnels buildings heating and cooling.

111 A first documented real-scale example of this innovative application is related to the Lainzer tunnel in Vienna  
112 (Adam and Markiewicz, 2009). During tunnel excavation by conventional NATM (New Austrian Tunnelling  
113 Method) tunnelling technique, a thermal activation trial was performed in lot LT22 in 2003. In particular, pipes  
114 were fixed to geosynthetics off site and then placed between the primary and the secondary lining. Hence,  
115 pipes laying can occur during the geotextile production process to streamline the installation phase on site. It  
116 consists of a full-fledged energy geotextile that was developed at Technische Universität in Vienna.

117 Another experience followed in Germany, where two 10 m-long sections of the Stuttgart-Fasanenhof urban  
118 railway link were equipped with an experimental geothermal plant (Schneider and Moormann, 2010). The  
119 monitoring results on a 4-years span are described in the works by Moormann et al. (2016) and Buhmann et  
120 al. (2016). The experimental campaign assessed the heat exchange potential, the impact of thermal loads on  
121 the subsoil and the influence of tunnel climate.

122 More recently, in China, some investigations (Zhang et al., 2013; Zhang et al., 2014; Zhang et al., 2016)  
123 focused on energy tunnels implementation. Indeed, in some regions of China such as Mongolia, average yearly  
124 temperatures are below zero degrees. To preserve the serviceability of infrastructures such as tunnels, lining  
125 and drainage, heating systems have to be installed so that absorber pipes withdraw heat from the inner tunnel  
126 sections and heating pipes deliver this heat at the tunnel portals. In this case, energy tunnels could replace  
127 traditional electricity-driven or coal-driven systems and thus reduce the high management costs on one side  
128 and decrease the carbon footprint. A full-scale example is the Linchang tunnel, in China, in the town of

129 Yakeshi, an autonomous region of Mongolia. Here the primary circuit is placed between the primary and the  
130 secondary lining 600 m away from the tunnel portal. The secondary circuit is close to the tunnel entrance  
131 between the secondary lining and an insulation layer, as well as in a ditch running parallel to the tunnel axis.

132 When it comes to open-cut tunnels, thermal activation can be achieved by equipping the diaphragm walls  
133 supporting the excavation and, possibly, the base slab with heat exchangers. Basically, the technology is the  
134 same as the one used for energy walls for urban excavations and/or foundations and support systems, for which  
135 many studies or real cases already exist in the literature (Amis et al., 2010; Bouazza et al., 2011; Sterpi et al.,  
136 2014; Bourne Webb et al., 2016; Di Donna et al., 2016; Barla et al. 2018a; Sterpi et al., 2018; Makasis and  
137 Narsilio, 2020; Zannin et al., 2020).

138 For tunnels built by mechanized tunnelling, the final lining is made of precast concrete segments mounted by  
139 the TBM within the shield protection. Precast segments are assembled to shape a ring, 1-2 m long. Typically  
140 every ring is made of 6-7 segments. In 2009 the first energy segments ring was tested in Katzenbergtunnel,  
141 before tunnel opening, where 5 segments were thermally activated for a total surface of 60 m<sup>2</sup> and a heat flux  
142 of around 10-20 W/m<sup>2</sup> (Franzius and Pralle, 2011; Moormann et al., 2016). Later, in the light of this experience,  
143 the technology was applied to the Jenbach railway tunnel in Austria, where 27 energy rings were conceived  
144 and built to cover the heat demand of the nearby city council (Frodl et al., 2010).

145 Other documented case studies can be found in Lee et al. (2012), who describes a testbed in Seocheon tunnel  
146 in Korea, or in Nicholson et al. (2014), for a potential application to Crossrail project's tunnels, Barla et al.  
147 (2016), Di Donna and Barla (2016), Bidarmaghz and Narsilio (2018) and Insana and Barla (2020), who studied  
148 the effect of soil thermal properties and of hydraulic flow on heat exchange, Cousin et al. (2019), who studied  
149 the application to Grand Paris tunnels, Tinti et al. (2017), with reference to the Mules Access Tunnel of the  
150 Brenner Base Tunnel (BBT) system, Makasis and Narsilio (2020) for the M4-M5 Link project in New South  
151 Wales in Australia, and Alvi et al. (2022) for the Lyon-Turin base tunnel. Peltier et al. (2019) and Dornberger  
152 et al. (2020) focused on the relevant role played in energy tunnels by the internal airflow characteristics (airflow  
153 temperature and velocity and heat transfer coefficient). Also Ma et al. (2021) analyzed the tunnel environment  
154 impact on energy tunnels' performance, finding that the temperature difference between tunnel air and heat  
155 carrier fluid is a key quantity, but attention should also be paid to the lining thermal properties. Recently, the  
156 thermo-mechanical behavior was investigated by Insana et al. (2020), Rotta Loria et al. (2022) and Ma et al.  
157 (2022) for the case of a coarse-grained soil.

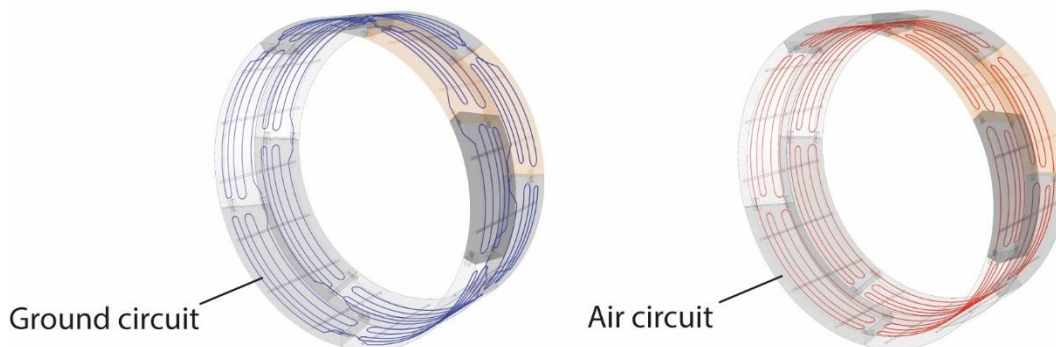
158 The arrangement of the tunnel for heat exchange takes place by equipping the lining with geothermal loops  
159 and by creating a connection plant with the collection and distribution network to the users, whether they are  
160 the stations themselves or the buildings at the surface. Nicholson et al. (2014) show a simplified conceptual  
161 framework of an exchange and distribution network to ground surface buildings devised for the Crossrail  
162 project, then never turned into reality. In their example, every building is provided with a heat pump. The  
163 overall system should include appropriate hydraulic pumps for heat carrier fluid circulation to and from the  
164 geothermal probes. Another solution could see a unique, centralized heat pump and a low-temperature

165 secondary distribution network towards the buildings. Both these options were studied for the application to  
166 the city of Turin and will be hereafter described.

### 167 **2.3 The Enertun technology**

168 The research carried out at Politecnico di Torino from 2013 onwards is particularly relevant for illustrating the  
169 milestones achieved, among which there is the development of a precast energy segment patent called Enertun  
170 (Italian patent number: 102016000020821, European patent number: 16834047.9) and the experimental  
171 campaign carried out in South Extension Line 1 Turin Metro tunnel (Barla et al., 2019b). The latter represents  
172 the first application of this technology in Italy and by far one of the most well-researched, especially by  
173 reference to the lining thermo-mechanical behaviour (Insana et al., 2020; Insana, 2020).

174 Thanks to an innovative layout of the geothermal probes, the Enertun energy segment reduces head losses by  
175 20-30% in each ring and increases its energy efficiency up to 10%. The same segment can be used to cool  
176 down the tunnel environment. There are three different configurations of the segment, according to the pipes  
177 mesh positioning, that is close to the extrados (Ground, Fig. 2.), close to the intrados (Air, Fig. 2.) or it can  
178 include two circuits, one per each of the previous locations (Ground&Air). In the first case the heat exchange  
179 with the ground is predominating, while it mainly involves air in the second case. In the third case, heat  
180 exchange can occur in both directions.



181  
182 Fig. 2 Ground and air Enertun configurations, which can be eventually combined together.

183

## 184 **3 DESIGN ASPECTS FOR ENERGY TUNNELS**

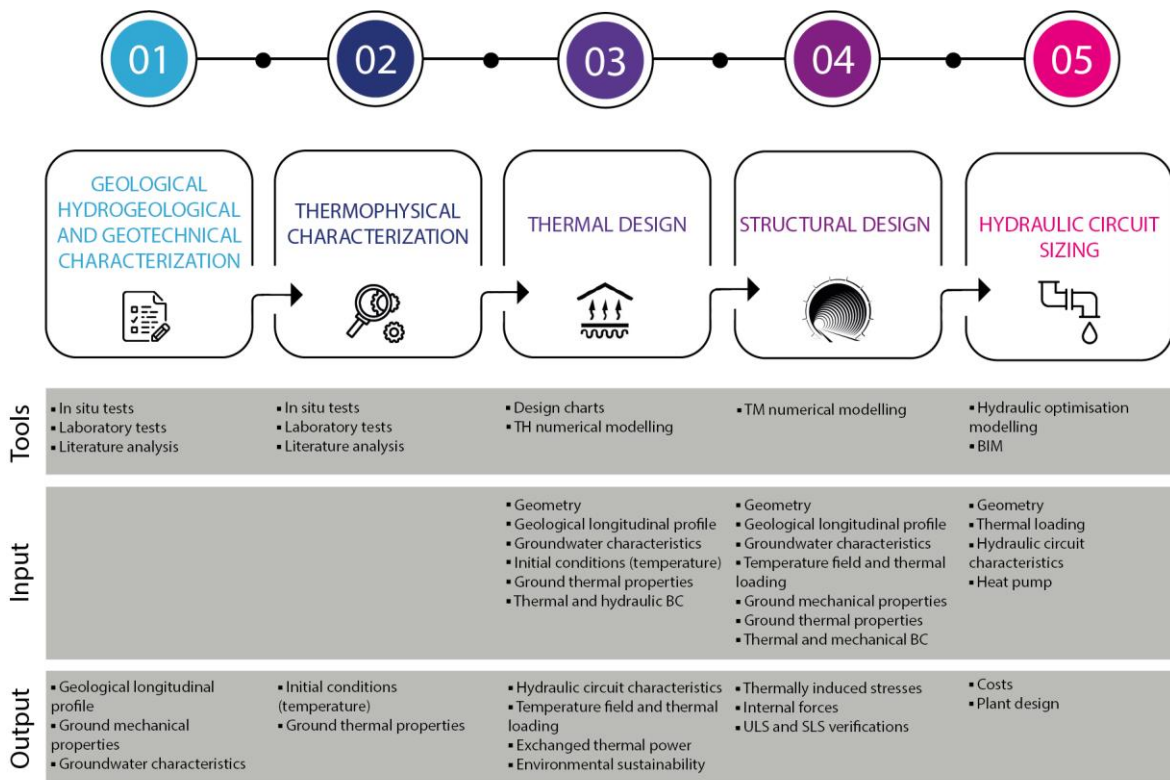
### 185 **3.1 General considerations**

186 The design process that leads to the realization of an energy tunnel goes beyond specific reference standards  
187 and cannot be merely reduced to a number of structural and/or geotechnical verifications. It necessarily  
188 encompasses a broad spectrum of issues that impact urban planning and the area energy procurement and  
189 distribution. The possibility to thermally activate a tunnel will have to be scheduled well in advance and since

190 the stage of an infrastructure feasibility study. Only then can it be guaranteed that the infrastructure contributes  
 191 to sustainable urban development thanks to its full integration into municipal energy planning.

192 Having said this, thermal activation of energy linings entails at least two technical aspects that need to be taken  
 193 into account during the project stages. An energy optimization analysis, aimed at maximizing the performance  
 194 under the same costs and evaluating the thermo-hydraulic interaction with the ground, is run first (thermal  
 195 design). This is followed by the structural design, that identifies the mechanical effects in the structural  
 196 elements following the thermal loading, assessed from previous stage, so that long-term integrity can be  
 197 guaranteed.

198 These aspects can be tackled through thermo-mechanical (TM) and thermo-hydraulic (TH) numerical  
 199 modelling respectively. Fully coupled thermo-hydro-mechanical (THM) simulations can be, initially, avoided  
 200 as in most cases the computational effort and the increase in calculation time are not reflected in a more  
 201 accurate result. For these reasons, in the following, the discussion will be limited to the illustration of results  
 202 stemming from TH and TM coupled analyses (Barla and Di Donna, 2018). A procedural proposal for the  
 203 design of energy tunnels was put forward during the works carried out at Politecnico di Torino (Baralis et al.,  
 204 2018; Barla et al., 2020) and is outlined in the flow chart in Fig. 3. It is highlighted that sizing of the hydraulic  
 205 circuit also needs to be carried out and will be described in the following.



206

207 Fig. 3 Design flow for an energy tunnel.

208

### 209 3.2 Thermal design

210 If structural design can be reasonably deepened later in the design stages, it is the thermal design that has to  
211 be addressed as early as the tunnel concept. The aim of thermal design is to quantify the heat power that can  
212 be extracted or transferred to the geothermal reservoir through the tunnel lining. This will depend on the  
213 specific in situ conditions, and will allow to assess the cost-effectiveness and the environmental sustainability  
214 of the system. The latter is about the evaluation of the effects of such systems on the surrounding environment,  
215 to limit their impacts as much as possible.

216 Because this is a relatively new technology, no clear methodological guidance or regulations exist for thermally  
217 sizing energy tunnels. Indeed, for other, more widely spread energy geostructures, such as foundation piles,  
218 the need to discuss about the introduction of design standards procedures, harmonizing them with the current  
219 regulatory framework, only recently showed up. In particular, some considerations on the need to introduce an  
220 approach consistent with limit state design emerged in the papers by Preene and Powrie (2009) and Bourne-  
221 Webb et al. (2014). As noted by these authors, the lack of codification is related to the fact that, so far, design  
222 was ruled by the experience cumulated during the implementation of traditional geothermal plants. For  
223 instance, referring to energy piles, it is common practice to simplify the problem to the case of a simple  
224 borehole heat exchanger (BHE). At the time of writing recommendations for designing and installing energy  
225 geostructures only exist in Switzerland (SIA, 2005), UK (GSHPA, 2012) and France (CFMS/SYNTTEC  
226 INGENIERIE/SOFFONS-FNTP, 2016). However none of them extensively treated energy tunnels.

227 First of all, following the flow chart in Fig. 3, supplementary investigations should be carried out, whose level  
228 of detail will depend on the design stage, aimed at assessing the ground thermo-hydro-geological  
229 characteristics that can influence the heat transfer processes (see Vieira et al., 2017; Vieira et al., 2022). The  
230 material parameters that have to be assessed are shown in Table 1.

231 Table 1 Ground and structural elements properties to be determined for thermal design of an energy tunnel.

Properties	Investigations
Thermal conductivity, $\lambda$ [W/mK]	TRT, needle probe, transient plane source
Thermal specific capacity, $S_c$ [J/kgK]	Transient plane source
Undisturbed temperature, $T_0$ [°C]	TRT, measures at different depths with level probe with temperature sensor
Effective porosity, $n_e$	Classification laboratory testing
Horizontal and vertical permeability, $k_h, k_v$ [m/s]	Pumping tests, slug test
Groundwater flow velocity, $v$ [m/s]	Level probe, existing groundwater maps
Groundwater depth, $f$ [m]	Level probe, existing groundwater maps
Groundwater flow direction, $df$	Level probe, existing groundwater maps

232

233 Among in situ testing techniques, the Thermal Response Test (TRT), very common for BHE and energy piles,  
234 is useful to evaluate ground thermal conductivity, heat exchanger thermal resistance and undisturbed ground

235 temperature. Laboratory testing can be classified into steady-state methods (e.g. hot guarded plate) and  
236 transient methods (e.g. needle probe, transient plane source) that allow assessing thermal conductivity, thermal  
237 diffusivity and volumetric heat capacity (ASTM, 2012; ASTM, 2014; Loveridge et al., 2017). However,  
238 laboratory measurements do not take into account site-specific conditions such as groundwater flow, spatial  
239 heterogeneity and scale effects that directly affect real thermal properties (Vieira et al., 2017).

240 To quantify the geothermal potential, a 3D thermo-hydraulic numerical model able to reproduce a portion of  
241 the thermally active lining has to be built. In the case of energy segments, a limited number of tunnel rings  
242 equipped with heat exchangers can be reproduced. In general, it is possible to refer to finite elements or finite  
243 difference codes.

244 Typically, the analyses reproduce the operation of the energy lining in correspondence of meaningful cross-  
245 sections for a certain number of years, to analyze not only short-term effects but also and especially long-term  
246 ones.

247 A detailed study of hydrogeological conditions is crucial to identify the groundwater regime. Indeed, in  
248 geothermal systems, the presence of a hydrodynamic flow plays a particularly favourable role in the heat  
249 transfer process given that it constantly recharges the reservoir from an energetic point of view thus preventing  
250 the geothermal resource depletion.

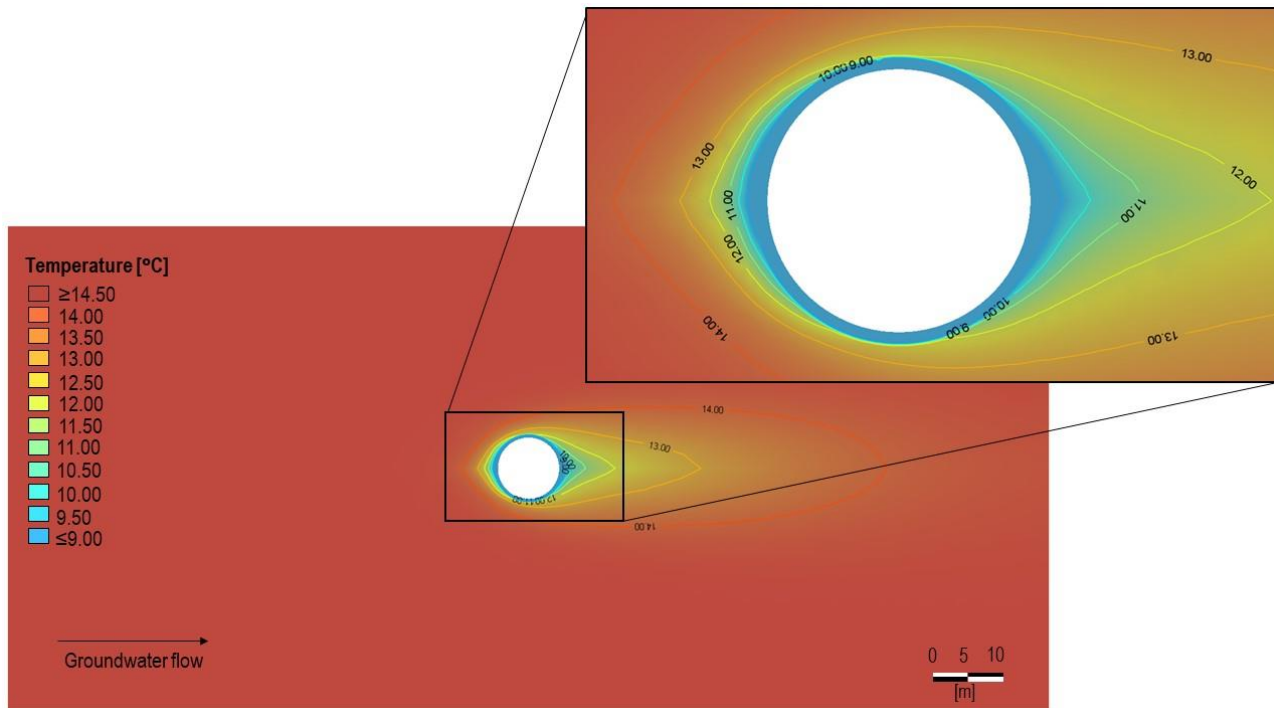
251 The TH analyses here presented as an example have been performed by means of the finite element code  
252 FEFLOW (Diersch, 2009). The thermo-hydraulic problem is dealt with by solving mass and energy  
253 conservation equations, by assuming Darcy's law for groundwater flow velocity.

254 To build the numerical model the correct case study geometry has to be accurately reproduced, including the  
255 layout and the geometry of the geothermal circuit and the ground thermal and hydrogeological conditions. In  
256 the example shown in Fig. 4, corresponding to a circular tunnel excavated in a saturated sand and gravel  
257 subsoil, groundwater flow was reproduced by setting a hydraulic head difference as boundary conditions on  
258 the lateral sides of the model, thus leading to a perpendicular flow with respect to the tunnel axis whose velocity  
259 depends on the ground permeability. Heat exchangers are simulated thanks to monodimensional elements  
260 implemented in the software. The use of these elements to represent geothermal installations pipes was  
261 validated and showed good consistency with data from analytical models (Diersch, 2009). Mass and energy  
262 conservation laws are fulfilled for these elements as well and the flow within them can be described by the  
263 Hagen-Poiseuille law. Hence, it is assumed as being in pure translation and with constant velocity.

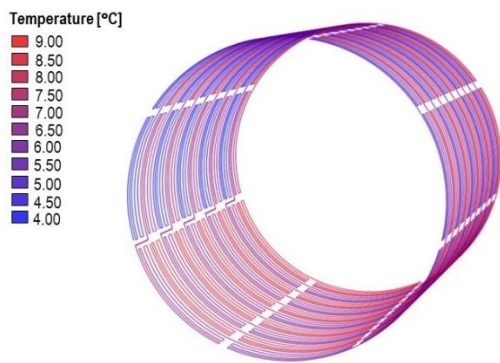
264 After setting initial conditions, the analysis is carried out by fixing inlet temperature and inlet/outlet velocity  
265 in the circuits and monitoring outlet temperature, function of the heat transfer which is reproduced numerically  
266 during the simulation.

267 By changing inlet temperature, the analysis can simulate the system behaviour during the different thermal  
268 activation seasons. For instance, if inlet temperature ranges from 24 to 28°C, summer operation is simulated,  
269 when excess heat is dispersed in the ground. Conversely, by setting inlet temperature between 3 and 6°C, it is

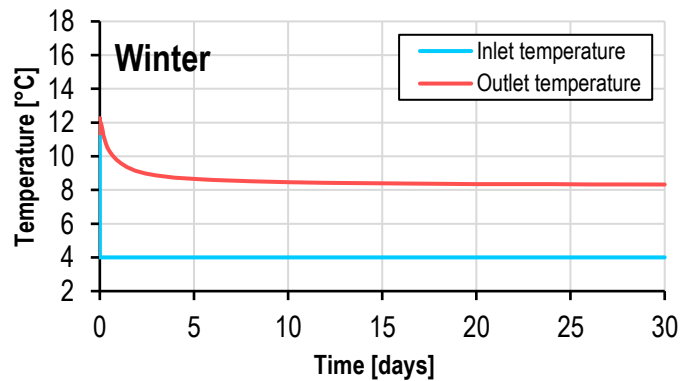
270 possible to simulate winter operation, characterized by heat extraction from the ground. This is shown in Fig.  
 271 4 where a typical winter result for the Torino case study is displayed in terms of soil temperature profile around  
 272 the tunnel and within the pipes and inlet/outlet temperatures computed. If inlet temperature varies cyclically,  
 273 according to the yearly operation, the seasonal plant functioning is simulated and long-term effects can be  
 274 assessed.



(a)



(b)



(c)

275 Fig. 4 Example of results for winter operation: soil temperatures a), pipes temperatures b) and energy segments inlet/outlet  
 276 temperatures c).

277 The heat power  $Q$ , expressed in W, exchanged during winter and summer can be computed from the difference  
 278 between pipes inlet and pipes outlet temperatures  $T_{wi}$ ,  $T_{wo}$ , according to the following formulation:

$$Q = mc(T_{wo} - T_{wi}) \quad (1)$$

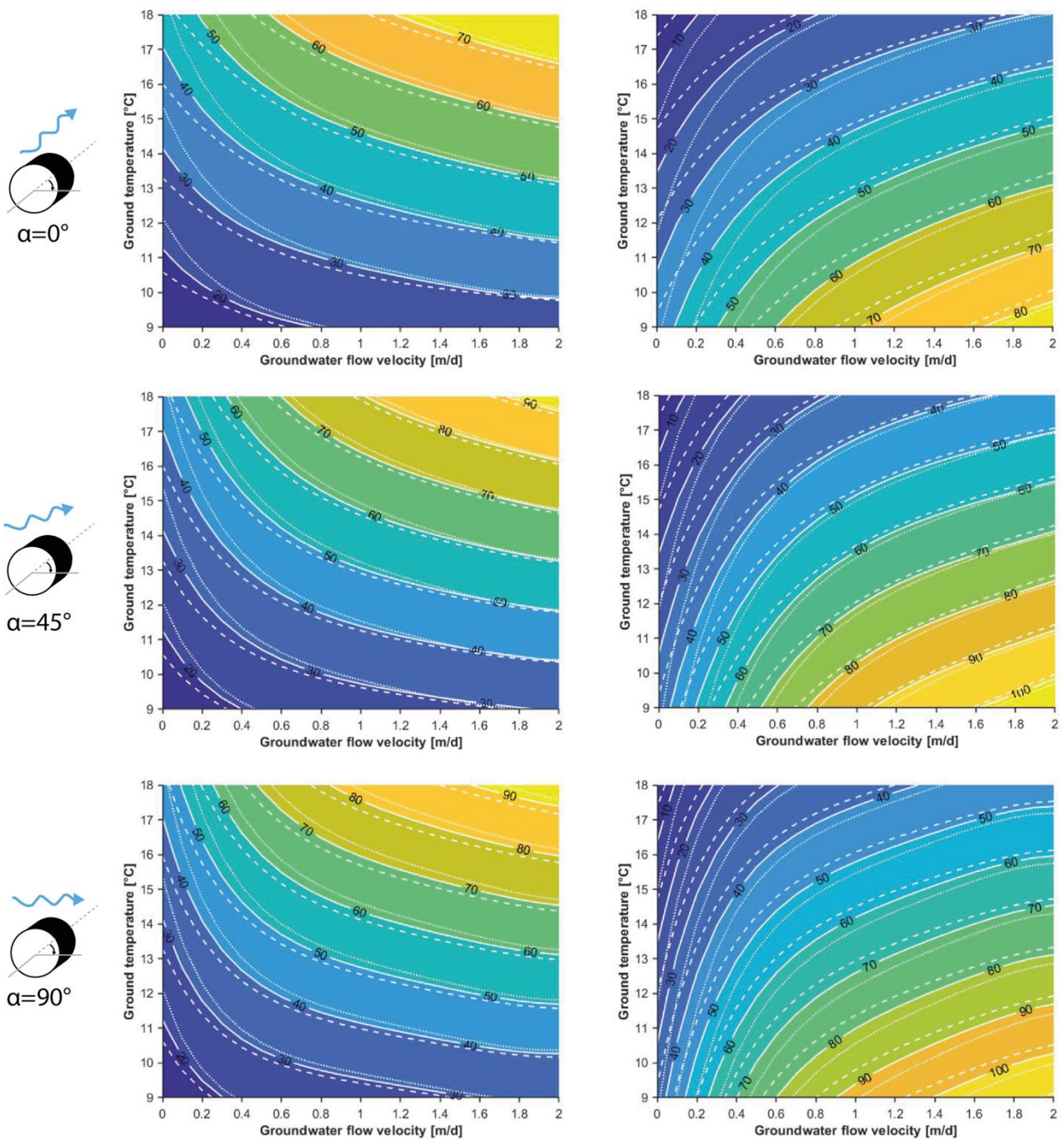
279 where  $m$  is the flow rate in kg/s and  $c$  is the heat carrier fluid heat capacity. Equation (1) enables to compute  
280 the heat exchanged for a specific case, then used for assessing the geothermal potential of the concerned part  
281 of the tunnel.

282 Another alternative approach was proposed by Delerablee (2019). It is based on the Gauss's theorem  
283 (divergence theorem) and allows to identify the heat exchanged by each control volume in the numerical model  
284 by conduction and by convection.

285 As already mentioned, several factors affect heat exchange. As a first approximation, to save time and avoid  
286 complete numerical modeling, Di Donna and Barla (2016) carried out a parametric analysis to study the  
287 influence of some key parameters such as ground temperature, groundwater flow and ground thermal  
288 conductivity. The work led to developing design charts to assess system energy efficiency according to the  
289 specific site conditions. Later, design charts were updated by Insana and Barla (2020) to account for the  
290 favourable configuration of the Enertun segment. The latter charts are more comprehensive as they also  
291 consider groundwater flow orientation with respect to the tunnel axis and heat carrier fluid inlet temperature  
292 thanks to a correction formula. These design charts are shown in Fig. 5 for winter and summer operations, as  
293 well as for three different groundwater flow directions. The specific heat power in  $\text{W/m}^2$  is obtained from a  
294 triplet of data, that is groundwater flow velocity (x-axis), ground initial temperature (y-axis) and total thermal  
295 conductivity (different lines hatchings). The results obtained showed good agreement with real monitoring  
296 data available in the literature pertaining to some of the sites described in chapter 2. Therefore, they can be  
297 used for a preliminary assessment of the heat exchanged. Further study will be needed at a later stage of design  
298 by performing specific numerical analyses for the specific application, as set out above.

### Winter-heat extraction

### Summer-heat injection



299

.....  $\lambda=0.9 \text{ W/(mK)}$     ———  $\lambda=2.26 \text{ W/(mK)}$     - - - - -  $\lambda=3.9 \text{ W/(mK)}$

300  
301

Fig. 5 Example of design charts for the definition of geothermal potential in  $\text{W/m}^2$  in winter and summer for multiple groundwater flow directions ( $0^\circ$ ,  $45^\circ$  and  $90^\circ$ ) (Insana and Barla, 2020).

302  
303  
304  
305  
306  
307

From the analysis of the design charts some general comments on energy tunnels behaviour can be drawn. No matter the flow direction, the highest performance is obtained with maximum ground thermal conductivity, maximum groundwater flow, due to the thermal recharge mechanism that allows the ground to return more rapidly to its undisturbed temperature, and with maximum ground temperature in winter and viceversa in summer. As groundwater flow velocity decreases, thermal conductivity starts playing a role. For perpendicular groundwater flow winter energy performance is in the range  $10\text{-}95 \text{ W/m}^2$ , while summer energy performance

308 falls between 10-110 W/m<sup>2</sup>, slightly higher than in summer. By observing the effect of groundwater flow, it is  
309 inferred that the performance is significantly increased when the flow is perpendicular to the tunnel axis as  
310 compared to an orientation of 0°, whereas little improvement is attributable to perpendicular flow in  
311 comparison to the oblique case.

312 Environment sustainability analysis completes the thermal design. This analysis aims to check potential  
313 impacts of tunnel energy lining on the surrounding environment, assessing the entity of thermal anomalies  
314 induced in the groundwater and the ground for different working hypotheses (winter only, summer only or  
315 both). Indeed, continuous winter operation could progressively decrease ground temperature leading to drift  
316 in time with resulting consequences not only on the following heating season but also on the balance of the  
317 surrounding ecosystem. This contingency has to be thoroughly examined taking into consideration, wherever  
318 possible, the operation for both heating and cooling. To this end, thermo-hydraulic numerical modeling can  
319 help too. As highlighted in Barla et al. (2016), the solution with lower environmental impact is achieved with  
320 geostructures working both in summer and in winter, where, at best, the amount of heat extracted in winter is  
321 balanced by the amount of heat stored during summer. In this way, a heating or cooling trend of the geothermal  
322 reservoir is largely reduced. However, this is not always in line with local energy demands and the  
323 environmental analyses should consider the real needs and the geostructure operation. Interaction with the  
324 surrounding environment and other possible uses of the resource have to be studied as described by a number  
325 of Authors (Bidarmaghz et al., 2017; Barla et al., 2018b; Epting et al., 2020).

326 Lastly, one of the peculiarities that can significantly affect the system's performance is tunnel climate, as  
327 pointed out by several Authors (Moormann et al., 2018; Nicholson et al., 2014; Peltier et al., 2019; Ogunleye  
328 et al., 2020; Dornberger et al., 2020; Ma et al., 2021). Heat exchange has been found to depend also on the  
329 difference between tunnel air temperature and the circulating fluid temperature and on airflow velocity  
330 (associated with the convection heat transfer coefficient). Thereby, knowledge of tunnel environment  
331 characteristics is a fundamental precondition for evaluating energy efficiency and technical-economic  
332 feasibility and can be accounted for, as done in this study, by means of a Cauchy boundary condition. Should  
333 this not be possible, various alternative scenarios can be considered in the coupled thermo-hydraulic analyses.

### 334 **3.3 Structural design**

335 The goal of structural design for energy tunnels is to examine the effects that thermal activation involves on  
336 the stress state in the lining, illustrating additionally the implications on structural dimensioning, if any. This  
337 is consequent to the change in internal actions caused by the change in the state of stress. In particular the key  
338 aspect is the quantification of the effect that thermal change, due to the fluid circulation within pipes in the  
339 lining, induces in terms of stresses. Once this is done, the influence on internal actions can be ascertained and  
340 the lining structural design can be updated, accounting for the loading scenario associated with the operation  
341 of the geothermal heat exchanger. Indeed, lining thermal activation can be treated as an additional loading  
342 stage compared to those ordinarily looked at during design.

343 With reference to energy geostructures in general, recommendations of some European societies (see GSHPA,  
344 2012) provide suggestions for the assessment of the additional thermal stress and/or strain state for energy  
345 piles. No specific directions can be found for tunnels. A detailed work in this perspective was performed by  
346 Insana (2020) who relied on experimental data and numerical analyses to understand the trends and the order  
347 of magnitudes of stresses and strains variations in the concrete lining in different directions based on the  
348 experimental campaign performed in the Turin Metro Line 1 full-scale test site, both in the natural state and  
349 under the particular conditions experienced upon thermal activation. Based on such findings with reference to  
350 a coarse-grained soil, upon cooling (winter heating mode) temperature decrease in the lining in the conditions  
351 studied is in the order of 4-6°C with subsequent contractive hoop strains of some tens of microstrain and a  
352 decrease in compressive stresses in the order of the MPa. The opposite behaviour is exhibited upon heating  
353 (summer cooling mode) with expansive hoop strains and an increase in compressive stresses, though in this  
354 case experimental data indicate an order of magnitude of some MPa. Moreover, the correlation of strains and  
355 stresses with temperature highlights an almost reversible behaviour with ranges of strains between  $\pm 100 \mu\epsilon$   
356 and of stresses between -2 and 3 MPa when temperature changes are  $\pm 8^\circ\text{C}$ . Strain temperature ratio is about  
357  $10 \mu\epsilon/^\circ\text{C}$ , very similar to the concrete thermal expansion coefficient, whereas stress temperature ratio goes  
358 from 0.1 up to 0.5 MPa/ $^\circ\text{C}$ . Longitudinal stress is null in all cases, showing a plane stress condition.

359 The problem can be investigated into more detail by resorting to numerical modeling. To analyze the energy  
360 lining working condition, a numerical model with thermomechanical formulation is needed, that allows to  
361 couple the mechanical and thermal aspects. Mechanical and thermal parameters of the materials involved will  
362 be derived from appropriate investigations and testing, as depicted in Fig. 3. The parameters of deformability  
363 and strength, the stress history of the site and what is necessary for a typical geotechnical calculation will have  
364 to be determined. Furthermore, the determination of the linear and volumetric thermal expansion coefficient  
365 for the materials involved (e.g. soil, concrete, filling grout) will be needed.

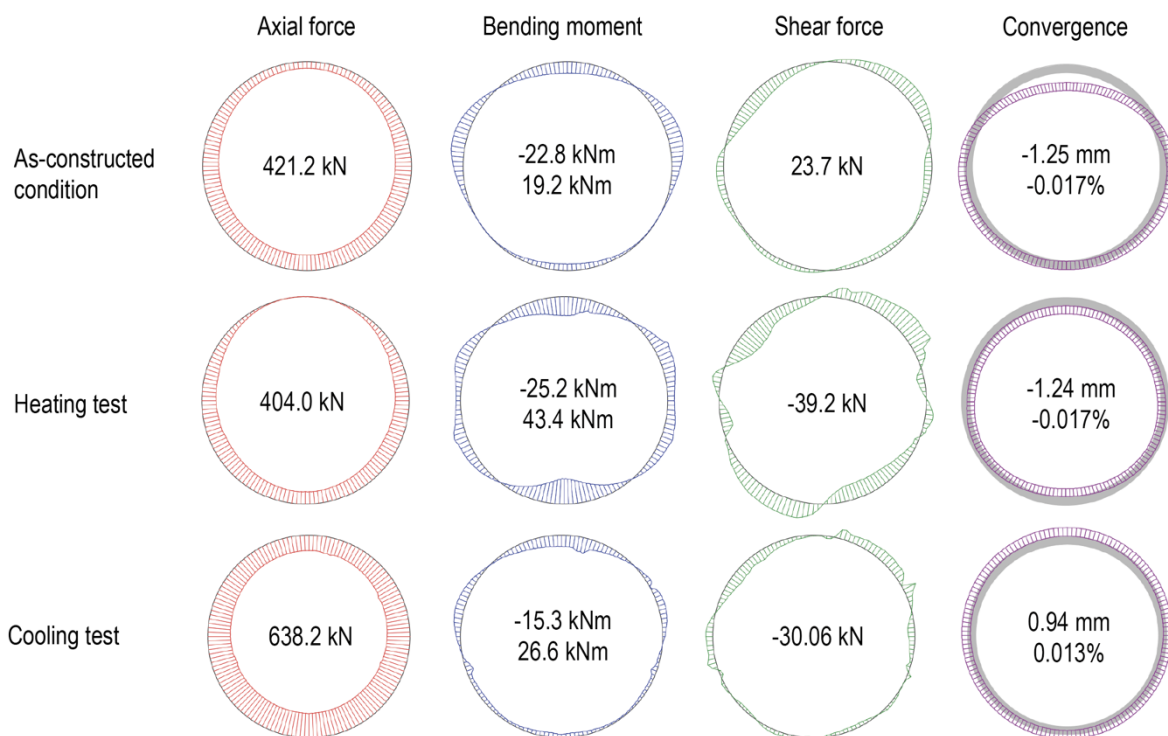
366 The numerical model will be such as to reproduce the different construction phases of the tunnel until  
367 commissioning, adding the heat exchange pipes, and an appropriate law of variation in temperature that  
368 reproduces the functioning of the system both in winter and in summer.

369 In particular, referring to a geothermal system with the double role of heating and conditioning, the structure  
370 will be prone to temperature variations during the several seasonal cycles that can trigger internal stress state  
371 changes. Such changes can give rise to a stress reduction, that is a compression, or to a stress increase in  
372 tension. In view of these aspects, the structural element reinforcement can be calculated. Fig. 3 explains this  
373 process schematically.

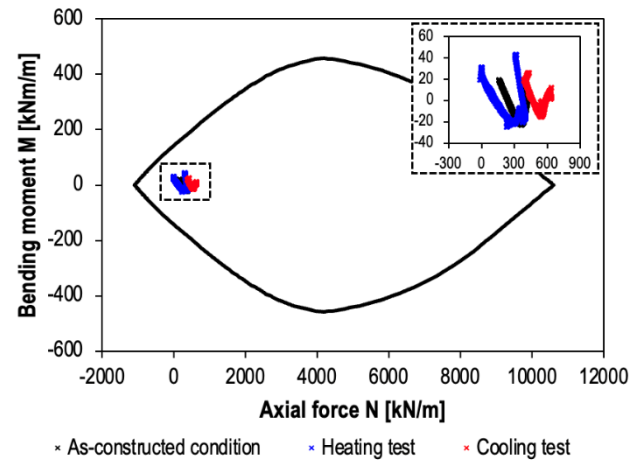
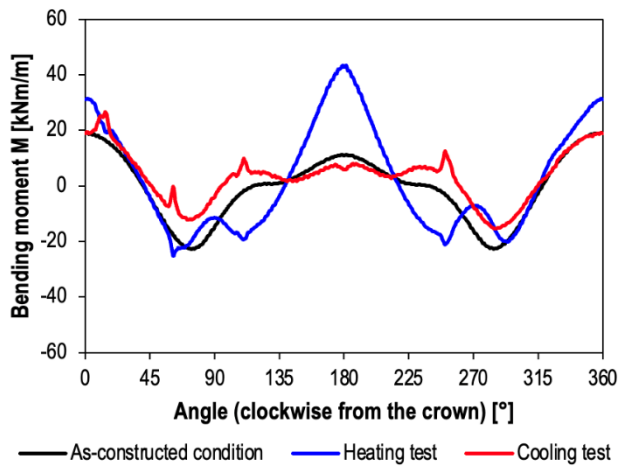
374 A calculation example for the assessment of internal actions and deformed tunnel shape in the energy rings of  
375 a metro tunnel after a heating and a cooling test is shown in Fig. 6 (Insana et al., 2020; Insana, 2020). In this  
376 case, thermo-mechanical analyses reproducing soil-structure interaction were carried out using the finite-  
377 difference software FLAC (Itasca, 2016). In these simulations, the heat transfer mechanism considered is  
378 purely conductive and the mechanical calculation is coupled to the thermal one with the purpose to quantify

379 thermally-induced stresses and strains. Coupling takes place in one direction only, that is stresses and strains  
 380 do not have an impact on thermal equilibrium. This simplification is completely acceptable as energy changes  
 381 for quasi-static mechanical problems are usually negligible.

382 In the example shown in Fig. 6 it follows that internal action changes with respect to those at the end of tunnel  
 383 construction are low and that axial forces and bending moments are largely included within the interaction  
 384 domain. The results obtained in the study illustrate that thermal loads acting on tunnels in alluvial soils involve  
 385 measurable and quantifiable effects. However, these effects are not considered to threaten the structural  
 386 integrity nor the serviceability of the lining and in the case analyzed, representative of a typical case study, no  
 387 need to increase steel reinforcement area or to modify the geometry of the cross section already defined based  
 388 on the traditional structural design was encountered. Besides, stress and strain changes associated with thermal  
 389 activation are of the same order of magnitude as those related to the seasonal temperature trend. However this  
 390 consideration does not undermine the need for additional structural verification since thermal cycles, albeit  
 391 similar to the natural ones, are imposed within the structures cyclically depending on thermal loads established  
 392 by the users, allegedly for the whole infrastructure lifecycle and could be of higher magnitudes for example if  
 393 energy tunnels are coupled to solar energy for storage purposes.



a)



b)

c)

394 Fig. 6 Internal actions in the energy rings (numbers refer to maximum values) at the end of construction and after a heating and a  
 395 cooling test a), detail of the bending moment b) and interaction domain c).

### 396 3.4 Hydraulic network sizing and preliminary cost analysis

397 Another design point covers the sizing of the hydraulic network for circulating the heat carrier fluid and for  
 398 connecting the primary circuit to the heat pump. Nicholson et al. (2014) assumed an hydraulic network with  
 399 return inverse arrangement with five neighbouring rings connected longitudinally to form one circuitry with  
 400 reference to the Crossrail project in London. Research carried out at Politecnico di Torino (Rosso et al., 2021)  
 401 showed that the most cost-effective layout is obtained by balancing the primary circuit installation cost,  
 402 increasing with circuitry cross-section, and pumping costs, decreasing with circuitry cross-section. Such  
 403 balance is highly affected by economic factors (e.g. pipes installation costs, energy cost), thermal comfort (e.g.  
 404 utilization rate of the heat exchanger) and plant-related factors (e.g. pipes length and heat carrier fluid  
 405 temperature changes). Hence, optimization of the hydraulic network has to be defined according to the specific  
 406 application, based on a cost-benefit analysis accounting for the above-mentioned technological aspects, site  
 407 geometry and potential customers identification.

408 Implementation costs for energy geostructures are lowered because the concrete members are already required  
 409 for structural reasons and do not need ad hoc excavations or drillings as for BHEs. Costs evaluation comes  
 410 down to assessing the extra costs (both materials and workmanship) needed for thermal activation beyond  
 411 those for building the geostructure.

412 For precast segmental lining, the cost of materials is related to PE-Xa pipes embedded in the lining, junctions  
 413 and further piping for guaranteeing hydraulic connections between segments and the circulation and  
 414 distribution to the heat pumps. As for workmanship, the process introduces some additional activities, such as  
 415 pipes embedment in the precast segments. This task takes place in the precast concrete plant with a slightly  
 416 higher burden of the workforce for laying pipes inside reinforcement and arranging pockets for linking  
 417 segments to one another. After tunnel excavation and rings erection, for which there are no increases in time  
 418 or costs, the segments of each ring will be connected to set up a closed hydraulic loop and header pipes will  
 419 be installed for ensuring the flow.

420 The analysis of such costs necessarily depends on the specific application, being a function of tunnel diameter,  
421 segments size, plant length, construction site organization, etc. Therefore, it is reasonable to evaluate the  
422 impact in percentage terms compared to the building costs of the tunnel itself. Based on the literature available  
423 and, particularly, in the light of the direct experience related to the experimental site in Turin Metro Line 1  
424 tunnel, this percentage can be estimated at 1-2%.

425 The result of an optimization analysis accounting for the above-mentioned costs is shown in Fig. 7, where the  
426 revenue to costs ratio for variable parameters can be observed. This evaluation supposed an operation over 180  
427 days per year (that is winter heating only), 12 hours/day.

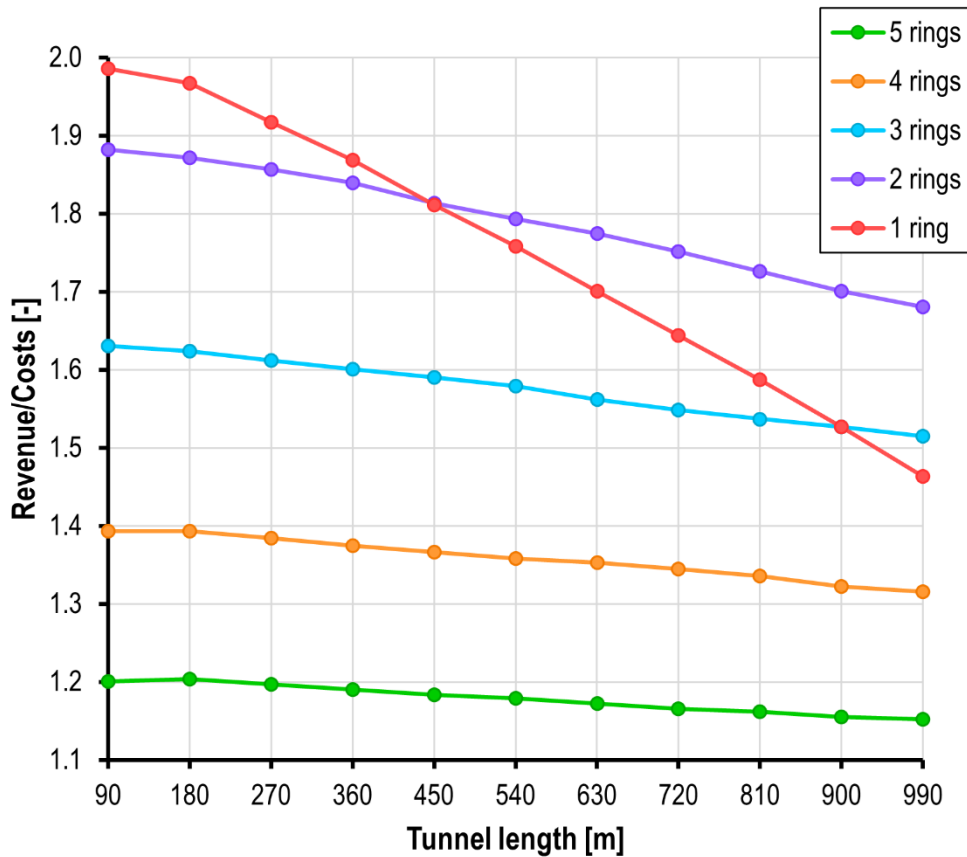
428 Revenues were obtained by means of thermo-hydraulic analyses that allowed to get the outlet-inlet temperature  
429 difference and, hence, the exploitable heat power for the Torino case study (Rosso et al., 2021). Accounting  
430 for the cost of 1 kWh<sub>t</sub> and for the operation time, the computed thermal power (in kW/m) was turned into the  
431 economic benefits deriving from the geothermal use of the tunnel lining. From this analysis the most  
432 convenient solution appeared to be that with all-in-parallel rings.

433 The hydraulic optimisation analysis considered the costs of the circuitry components and the costs for pumping  
434 the heat carrier fluid through the primary circuit. It calculated installation costs, head losses and hydraulic  
435 power, based on which the pumping energy cost was estimated. The minimum cost was found for the  
436 configuration with 5 rings in series.

437 Both the thermo-hydraulic and the hydraulic optimisation analyses carried out considered different plant  
438 solutions (from one to 5 rings connected in series to form one circuitry) and tunnel lengths from 90 to 990 m.  
439 The revenue to costs ratio was obtained by dividing the economic benefits and the hydraulic costs obtained as  
440 described above. From Fig. 7 it turns out that all-in-parallel rings is the best case up to 450 m. As tunnel length  
441 increases, the highest revenue is obtained with two rings in series.

442 It can be observed that the shortest tunnel length considered has the highest revenue to cost ratio regardless of  
443 the number of rings connected in series. This downward trend is because the hydraulic cost increase rate is  
444 higher than the thermal gain increase rate when tunnel length increases, hence for higher lengths the revenue  
445 to cost ratio decreases.

446 The results discussed are not of general validity, being related to the economic value of the heat and to its  
447 exploitable amount, which, in turn, is a function of boundary conditions in terms of groundwater flow,  
448 lithology, tunnel climate, pipes inlet temperatures and so on. Nevertheless, they are suggestive of the kind of  
449 economic assessment needed and of energy tunnels cost-effectiveness.



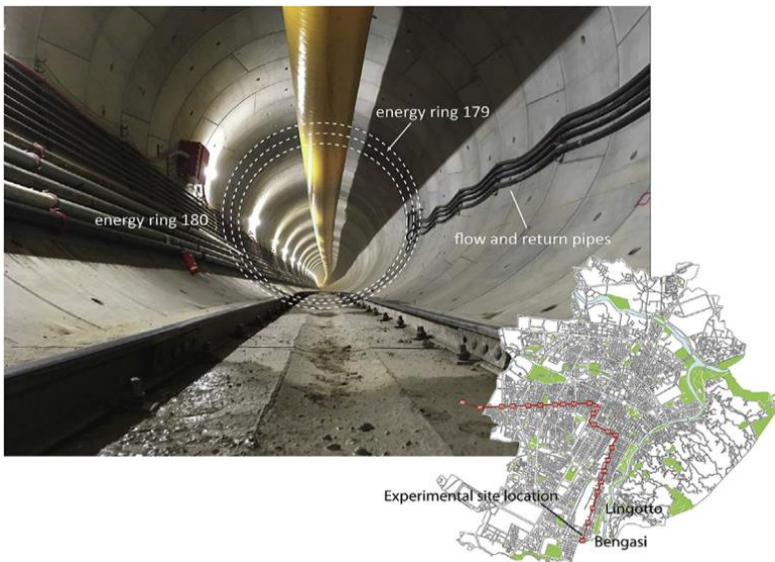
450

451 Fig. 7 Revenue to costs ratio for different configurations and tunnel lengths (operation over 180 days, 12 hours per day).

452

453 **4 TURIN METRO LINE 1 PILOT SITE**

454 After the description of design aspects, it is of interest to describe in the following a real application of energy  
 455 tunnel. In order to verify the proper operation of the Enertun energy segment, a project for the construction of  
 456 an energy tunnel experimental prototype began in 2016 in the framework of a joint project between Politecnico  
 457 di Torino, InfraTo and Consorzio Integra. The prototype was installed in the Turin Metro Line 1 South  
 458 Extension tunnel during its construction (Barla et al., 2019b), about 42 m northwards from Bengasi station, in  
 459 the Lingotto-Bengasi section (Fig. 8). It consists of 12 Enertun segments (2 complete lining rings) equipped  
 460 with the Ground&Air configuration. The precast segmental lining is 30 cm thick and is made of 6 segments (5  
 461 plus a key). Each ring is 1.4 m long with an internal diameter of 6.88 m. The groundwater table is about 12 m  
 462 deep.



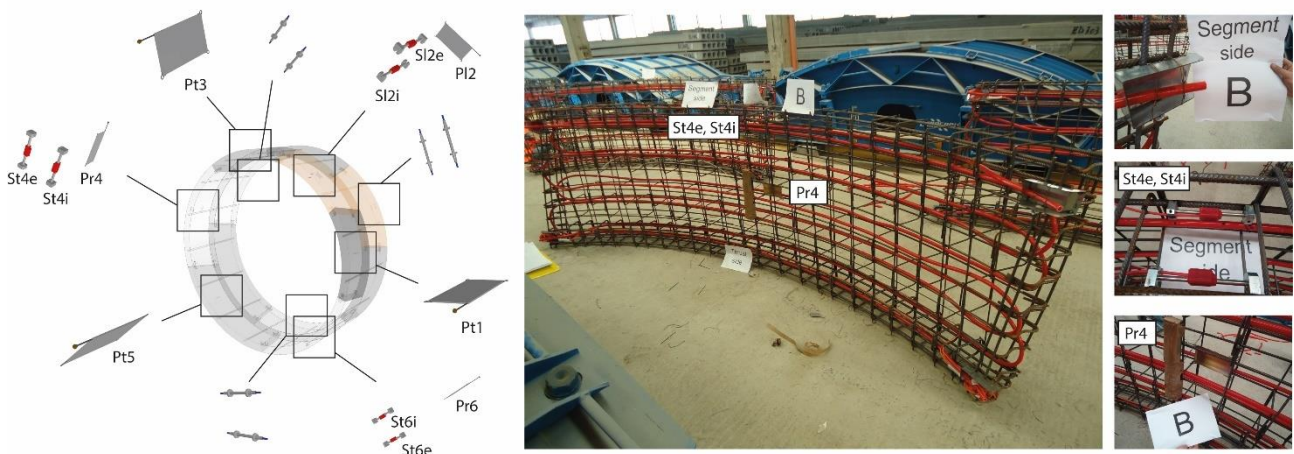
463

464 Fig. 8 View of the Enertun experimental site and its location along Turin Metro Line 1 (Insana and Barla, 2020).

465 Segments precasting took place between December 2016 and May 2017. Fig. 9 shows an example of a segment  
 466 before casting with geothermal loops fixed to reinforcement.

467 The rings were mounted by the TBM on-site in July 2017. Next, all hydraulic connections between segments  
 468 and with the heat pump were provided. All exposed pipes were suitably insulated to prevent heat losses. The  
 469 heat pump and fan coil were placed in the station area.

470 Given the experimental nature of the project, a complex and comprehensive monitoring system was installed  
 471 to help assessing the thermal and structural performance of energy segments (Fig. 9). The system includes  
 472 stress, strain and temperature gauges embedded within segments before casting, temperature probes along  
 473 pipes, flow meters and heat meters.



474

475 Fig. 9 Measurement sensors arrangement in the two energy rings and view of an energy segment before casting.

476 Testing started in September 2017 and lasted one year, allowing to study the winter and summer behaviour,  
 477 for a total of 12 tests, using both the Ground and the Air exchange circuits. The results of the campaign helped

478 to quantify heat exchange ranging from 40 to 66 W/m<sup>2</sup> based on the type of application (see Barla et al., 2019  
479 and Insana and Barla, 2020). The impact of thermal loads on the lining stress-strain state resulted very limited  
480 (Insana et al., 2020).

481 The promising results obtained allowed to quantify the energy performance of the technology in the Turin  
482 context, paving the way for an application at a much larger scale, as described in the following chapter.

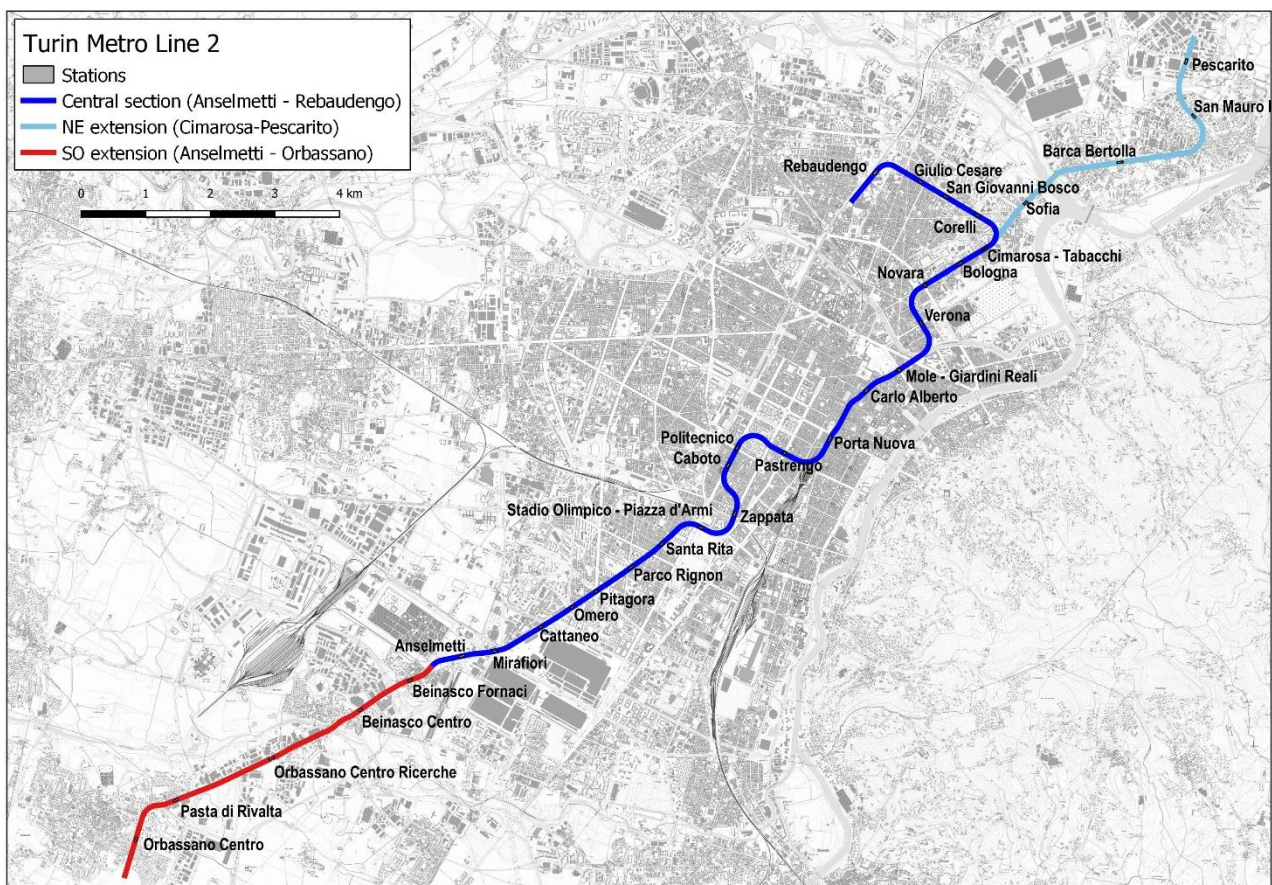
483

## 484 5 TURIN METRO LINE 2 APPLICATION

### 485 5.1 General features

486 In the framework of the technical and economic feasibility study for the design of Turin Metro Line 2, a study  
487 on the geothermal potential of the tunnel infrastructures along the line was carried out. As anticipated, this is  
488 the first study ever involving the whole metro line as a possible source of heat (Barla et al. 2019a; Barla et al.,  
489 2020).

490 The entire route of the line, as detailed in the technical-economic feasibility project, will be composed of a  
491 central section winding between the Anselmetti and Rebaudengo stations (blue line in Fig. 10) and two  
492 extensions, respectively NE (light blue line) and SW (red line).



493

494 Fig. 10 Turin Metro Line 2 plan.

495 The central section will cross the city underground for 15.7 km with a rather complex trend. The altimetry of  
496 the tunnel includes several and sudden variations along the route with the rail level placed from a minimum of  
497 about -10 m in the northern area, between Corelli and Giulio Cesare stations, up to -40 m from ground surface  
498 near the Zappata Station below the railway link.

499 Based on the path described above, tunnel excavation between Anselmetti and Bologna stations is planned to  
500 be performed by mechanized excavation with TBM, while the terminal northern stretch of the central section  
501 between Bologna and Rebaudengo will be carried out by the Cut & Cover excavation methodology (C&C) or  
502 with artificial box. The C&C method will be also adopted for the SE junction building near Cattaneo station.  
503 The conventional excavation methodology will be used for a short section between Zappata and Caboto  
504 stations to underpass the railway link that connects the stations of Porta Nuova and Porta Susa. The 5.7 km  
505 long NE extension will be built by means of mechanized excavation with TBM, except for a short initial and  
506 final section, both built by C&C technique. The whole SW extension will be excavated by TBM.

507 Two different structural types which can be thermally activated emerge from the above: i) lining made of  
508 precast reinforced concrete segments in the tunnel sections built by TBM; ii) cast-in-place reinforced concrete  
509 vertical diaphragm walls for the sections of the tunnel excavated by C&C or with artificial box and for stations,  
510 junction buildings and rear-end buildings.

511 The two sections planned with conventional excavation method are not considered suitable to thermal  
512 activation, based on technical and economic considerations.

## 513 **5.2 Homogeneous zoning**

514 The working methodology adopted to quantify the geothermal potential along the line chainage consisted of  
515 the following steps:

- 516 - geological and thermo-hydraulic characterization of the line for the assessment of the data needed for  
517 numerical modelling;
- 518 - zoning of the line into homogeneous sections;
- 519 - development of finite element numerical models with thermo-hydraulic coupling for evaluating the  
520 energy efficiency of the different tunnel sections;
- 521 - evaluation of the overall power in summer and in winter;
- 522 - study of potential customers.

523 Considering the heterogeneity of the route plan and altimetric trend, of groundwater level and of ground  
524 geological-geotechnical conditions, a specific parameterization methodology with distinction into class was  
525 developed and implemented on Open Source GIS systems. Through appropriate geoprocessing and map  
526 algebra operations it was possible to compare spatially the information pertaining to different sections of the  
527 line with the distribution and the plano-altimetric variation of the parameters taken into consideration. Together  
528 with these parameters, the excavation techniques are also considered by analyzing separately the sections of  
529 the tunnel that will be built by TBM and those that will be built with the C&C technique or artificial box.

530 For each of the two structural types, TBM and C&C, five parameters have been identified for the classification  
 531 of the different sections with regard to the ground geothermal potential:

- 532 - Position of the piezometric surface with respect to the tunnel;
- 533 - Groundwater temperature;
- 534 - Groundwater flow direction with respect to the tunnel axis;
- 535 - Groundwater flow gradient;
- 536 - Lithology around the tunnel.

537 Fig. 11 shows the matrices with all the classes obtained, for the sections excavated both by TBM and by C&C  
 538 respectively, which were adopted to zone the entire line in homogeneous sections. The parameters were derived  
 539 both from the analysis of literature (Bottino and Civita 1986; Barla and Barla 2012; Barla et al. 2015) and from  
 540 specific investigations carried out as part of the feasibility study.

541 For the whole development of line 2, based on the subdivision of the parameters into classes, 50 and 16  
 542 homogeneous sections were identified for the portions which will be excavated by TBM and by C&C  
 543 respectively. For each homogeneous section thus identified, a specific FEM thermo-hydraulic numerical model  
 544 was built to determine the geothermal potential of the corresponding tunnel section. Fig. 12 shows as an  
 545 example of some geometries of the numerical models for the TBM and C&C sections.

	Position of the piezometric surface with respect to the tunnel [m]	Groundwater temperature [°C]	Groundwater flow direction with respect to the tunnel axis [°]	Groundwater flow gradient [%]	Lithology around the tunnel
<b>Classes for the TBM sections</b>					
1	Above the crown	From 14 to 15	Perpendicular to tunnel axis $\pm 30^\circ$	> 0.40	Completely in sandy-gravel deposits <sup>1</sup>
2	Between crown and invert	From 15 to 16	Intermediate situation	From 0.40 to 0.25	At the contact between sandy-gravel deposits <sup>1</sup> and sand layers <sup>2</sup>
3	Below the invert	From 16 to 18	Parallel to tunnel axis $\pm 30^\circ$	< 0.25	At the contact between sandy-gravel deposits <sup>1</sup> and clay layers <sup>3</sup>
4	-	-	-	-	Completely in sand layers <sup>2</sup>
5	-	-	-	-	Completely in clay layers <sup>3</sup>
<b>Classes for the Cut &amp; Cover sections</b>					
1	Above the diaphragm wall median point	From 14 to 15	Perpendicular to tunnel axis $\pm 30^\circ$	> 0.4	Completely in sandy-gravel deposits <sup>1</sup>
2	Between the diaphragm wall median point and the wall base	From 15 to 16	Intermediate situation	From 0.40 to 0.25	The contact between sandy-gravel deposits <sup>1</sup> and sand layers <sup>2</sup> lies between the median point and the diaphragm base
3	Below the diaphragm wall base	From 16 to 18	Parallel to tunnel axis $\pm 30^\circ$	< 0.25	The contact between sandy-gravel deposits <sup>1</sup> and clay layers <sup>3</sup> lies between the median point and the diaphragm base

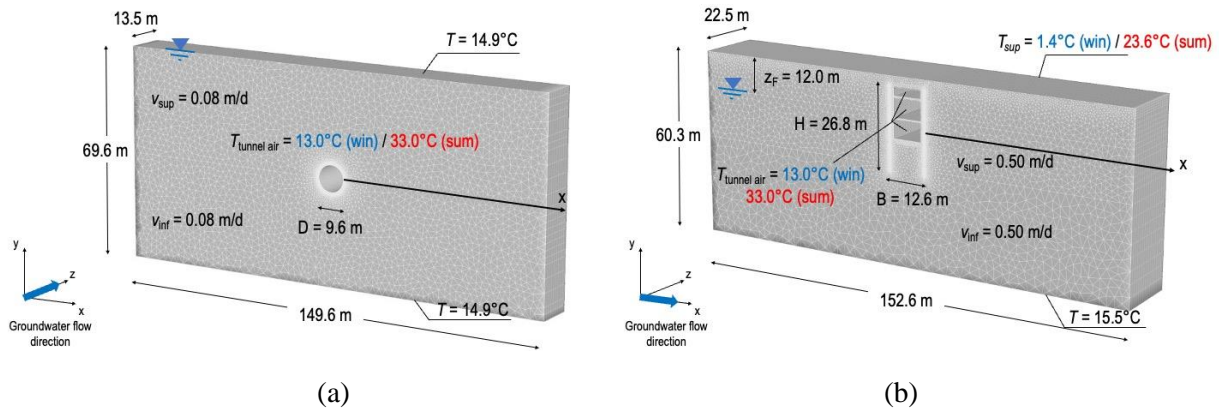
<sup>1</sup>  $k_h = 1.93 \cdot 10^{-3}$  m/s;  $k_v/k_h=0.05$ ;  $\lambda=2.7$  W/mK;  $\rho_c=2.6$  MJ/m<sup>3</sup>K;  $n_e= 0.175$

<sup>2</sup>  $k_h= 4.2 \cdot 10^{-4}$  m/s;  $k_v/k_h=0.05$ ;  $\lambda=3.3$  W/mK;  $\rho_c=2.5$  MJ/m<sup>3</sup>K;  $n_e= 0.125$

<sup>3</sup>  $k_h = 1 \cdot 10^{-8}$  m/s;  $k_v/k_h=0.05$ ;  $\lambda=1.7$  W/mK;  $\rho_c=2.3$  MJ/m<sup>3</sup>K;  $n_e= 0.05$

546

547 Fig. 11 Summary matrix for TBM and C&C sections with indication of the classes for the five parameters taken into account in the  
 548 proposed methodology.



549

550

551

552

Fig. 12 Example of numerical models' geometry adopted for TBM sections (a) and for C&C sections (b) with indication of thermal and hydraulic boundary conditions.

553

554

### 555 5.3 Computation of geothermal potential and identification of customers

556

557

558

559

560

From each finite element numerical analysis, it was possible to get the temperature difference between inlet and outlet of the heat exchanger in winter and summer. Such a result was used to calculate the specific thermal power in W/m, according to the procedure described in Chapter 3. Total thermal power in kW, for the specific homogeneous section, was then obtained by multiplying the specific thermal power per unit length by the length of the examined section.

561

562

563

564

565

566

567

568

Numerical analyses were carried out by simulating a 30-days thermal activation timespan, assumed as a conservative condition for the computation of the heat exchanged through the tunnel lining. Indeed, in this case the most unfavourable conditions in terms of heat carrier fluid inlet temperature and tunnel air, representative of peak hours as concerns passengers and trains frequency, are kept constant for the entire period of 30 days. This assumption, useful to allow the computation, clearly does not match real operation conditions, characterized by both a seasonal and a daily variation. Therefore, the conservative conditions considered in the analyses are likely to occur for few hours a day and for some days of the year, not for the whole timespan. However, this hypothesis was reputed appropriate at this stage of the design.

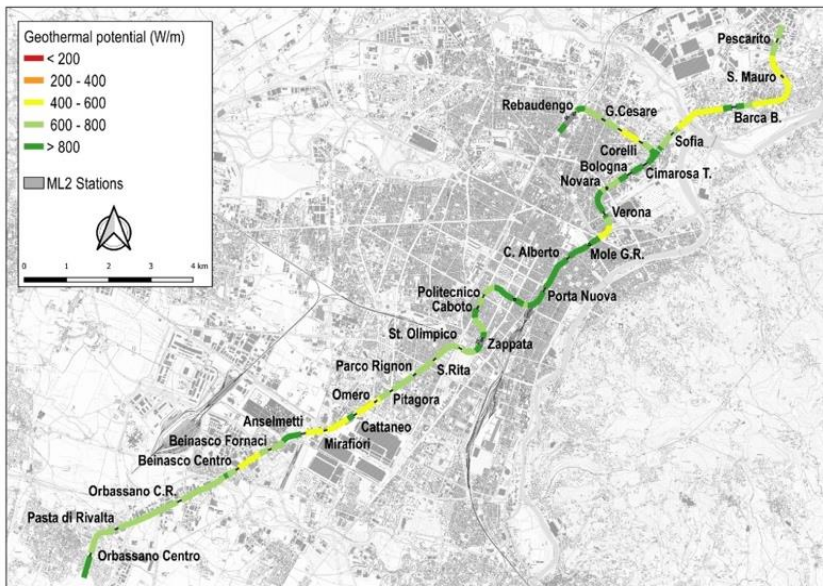
569

570

571

572

Results, referred to the last simulated day of thermal activation, allowed to quantify the exploitable heat along all the different sections of the tunnel and to classify them according to the geothermal potential ranging from 400 to 1200 W/m in the most unfavourable and favourable conditions respectively. Fig. 13 illustrates the classification of the line based on winter geothermal potential.



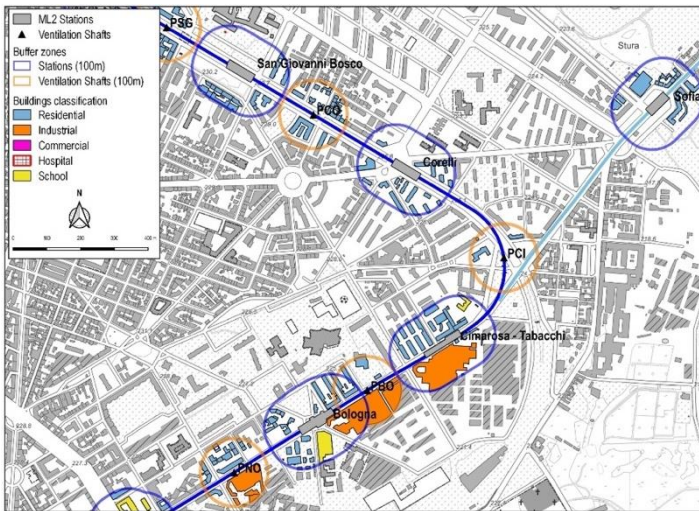
573

574 Fig. 13 Example of the line classification according to the winter geothermal potential (W/m).

575 The winter performance of the technological system was found to be better than the summer one. In particular,  
 576 the most productive areas were that below the historical city center and, at a larger scale, the central section,  
 577 followed, in the order, by the SW and the NE extension, both in summer and in winter. Up to 18.7 and 11.9  
 578 MW of thermal power respectively in winter and summer can be exploited along the line.

579 Based on the calculated thermal power and the distribution of potential receivers along the line, a proposal for  
 580 the use of heat was suggested which fulfils stations' winter and summer thermal needs. Then, any possible  
 581 surplus of thermal energy which can be distributed to external users was furtherly assessed. Its amount is  
 582 particularly interesting in winter but, especially in some areas, relevant in summer too. Considering that the  
 583 stations total thermal needs were evaluated to be of 6.2/7.5 MW (Winter/Summer), an interesting surplus  
 584 (12.5/4.4 MW) can be made available to the city district heating system or directly to external users.

585 Finally, to identify possible receivers of the heat exchanged by the tunnel lining, the contact points between  
 586 the thermally activated infrastructure and the topographic surface (i.e. stations and ventilation shafts) were  
 587 located. The stations were considered as polygonal elements while ventilation shafts were considered as simple  
 588 point elements to simplify the analysis. Starting from the contact points, buffer areas with a radius of 100 m  
 589 were defined around them, within which it is believed that distribution of thermal energy exchanged with the  
 590 ground would be possible (Fig. 14). Within these areas 1740 potential receivers (buildings) were identified, of  
 591 which 1045 around the stations and 695 around the ventilation shafts. Among them, some appear particularly  
 592 interesting, such as the school buildings along the route, the San Giovanni Bosco hospital, the new service  
 593 building for bus lines with commercial premises planned near Orbassano Centro Ricerche station and the newly  
 594 built areas adjacent to Rebaudengo station, Regaldi boulevard or the area behind the Fiat Mirafiori plants.



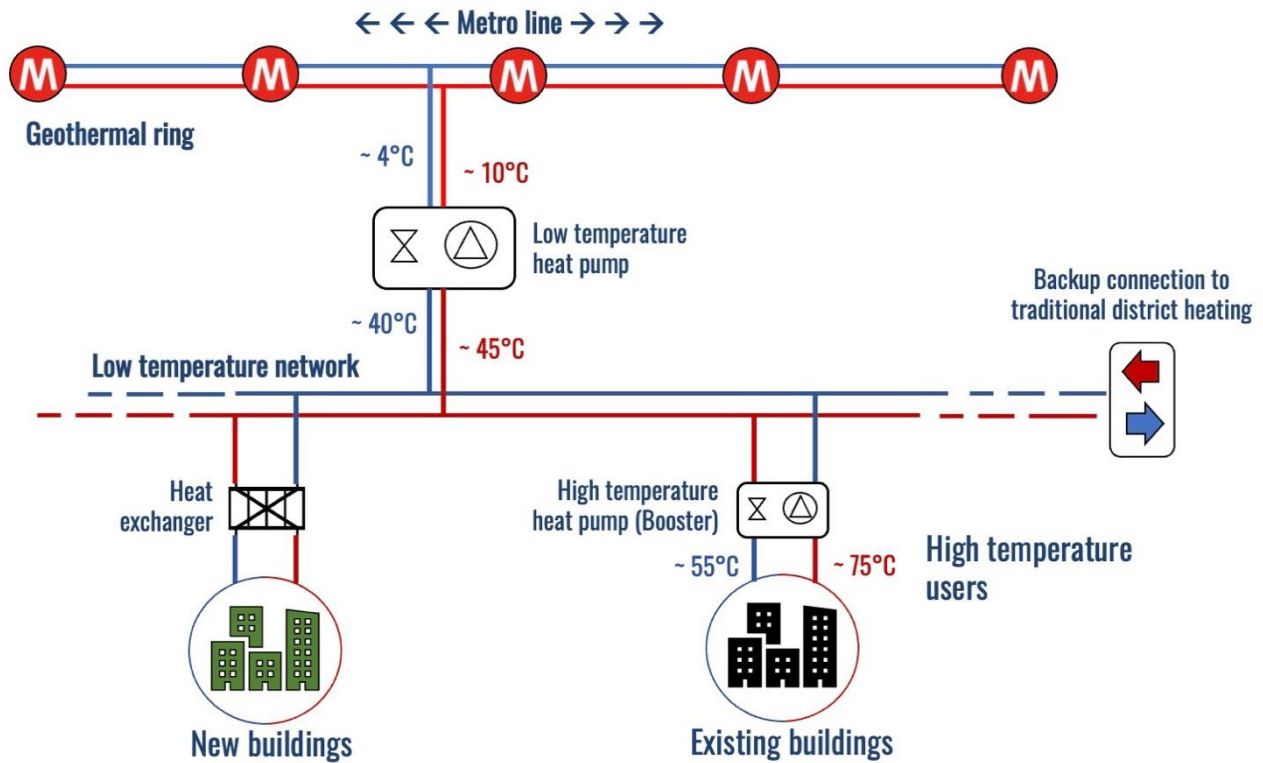
595

596 Fig. 14 Example of identification and classification of the potential receivers along the Novara-Giulio Cesare portion of the line.

597 **5.4 Integration with district heating networks**

598 If the extracted heat can be used directly for the line stations or with reference to specific receivers identified  
 599 among the surface buildings, an interesting possibility which was investigated in this study is to integrate the  
 600 energy tunnel system within the district heating network. In this case, a scheme like the one shown in Fig. 15  
 601 can be assumed. The tunnel (Geothermal Ring) plays the role of thermal source for the low-temperature ring  
 602 (Primary ring) through the use of a heat pump (Primary heat pump). The geothermal loop is then the source,  
 603 evaporator side, for the heat pump which raises the temperature from the tunnel operation levels (4-10°C) to  
 604 around 45°C. The primary network can thus serve directly the newly built volumes and, in general, the users  
 605 characterized by low specific consumption and equipped with low-temperature thermal plants (New Buildings  
 606 with radiant floor/fan coil in Fig. 15). This seems to be the most interesting use from a technical and economic  
 607 perspective. The use of heat pumps as heat sources for district heating or as boosters is common in northern  
 608 European countries such as Sweden, Netherlands or Denmark (Connolly, 2017; European Heat Pump  
 609 Association, 2019) while is limited in Italy. Accordingly, Meibodi and Loveridge (2022) state that the  
 610 connection of energy geostructures to the heat network, operating at different temperature levels, is a feasible  
 611 solution in the framework of the fifth generation thermal energy network's schematic concept.

612



613 Fig. 15 Conceptual scheme of the geothermal system.  
614

615 As to existing users and those that require high temperatures, it is possible to think of using a second local heat  
616 pump (Booster) to raise the temperature to the 75°C needed by radiators and ensure comfort. To guarantee  
617 service continuity and system resilience, it may be necessary to provide a connection with the high-temperature  
618 district heating network that can act as a backup in case of failures or maintenance of the network and/or the  
619 equipment.

620

## 621 6 CONCLUSIONS

622 The main advantage resulting from the integration of heat exchangers inside geotechnical structures lies in the  
623 fact that they are built in any case. This involves a significant reduction in installation costs, compared to the  
624 construction of a traditional geothermal plant. Thermal activation of the tunnel linings is therefore an excellent  
625 opportunity to mine the ground heat with great economic and environmental advantages.

626 The key aspects of the design process were illustrated in this paper making particular reference to the studies  
627 carried out at Politecnico di Torino from 2013 to date.

628 Compared to the structural dimensioning of the segments used for the lining, in the case of energy tunnels and,  
629 therefore, of energy segments, design requires two additional stages, identified as thermal design and structural  
630 design. The first one concerns the energy sizing of the heat exchanger system. Here the attention of the designer  
631 must be focused on the efficiency of the geothermal system, on the design of plants and on environmental

632 sustainability. The second one aims at quantifying the effects involved on the lining by the system thermal  
633 activation from a stress point of view. A third stage ,i.e. hydraulic circuit sizing, is also required.

634 Tunnels can get to about 10-20 W/m<sup>2</sup> of specific heat power exchanged in the absence of groundwater flow,  
635 up to 50-60 W/m<sup>2</sup> in case of relevant groundwater flow.

636 The use of tunnels as heat exchangers with the ground finds its best application in urban areas as described in  
637 this paper. Indeed, in this case, the extracted heat can be easily used to heat the neighbouring buildings and the  
638 plant can be integrated into urban district heating systems. In this perspective, careful urban planning is even  
639 more necessary to optimize interference between different systems and integration with distribution networks.  
640 The cities that will be able to address these issues will certainly be able to benefit from it in terms of life quality  
641 improvement. This paper described a study conducted in the city of Turin, which represents the first relevant  
642 example of the possible synergies that can be generated by adopting this technology at a large scale. Up to  
643 18.7 and 11.9 MW of thermal power respectively in winter and summer can be exploited along the line and  
644 used for satisfying the thermal needs of the stations and/or made available to the city district heating system.

645 As emerged, research in the field of energy tunnels is highly multidisciplinary and involves skills and  
646 disciplines that go beyond pure geotechnics, such as geology, hydrogeology, hydraulics. Broad-spectrum  
647 cooperation is needed, with colleagues dealing with energy, hydraulic and environmental engineering,  
648 management engineering and public and urban planning policies in order to overcome the obstacles that still  
649 hinder the full use of this technology.

650 Energy tunnels represent a potential element of technological innovation for the years to come, in line with  
651 environmental sustainability policies and it is very nice to think that this push comes from geotechnics, a  
652 discipline sometimes seen as very traditional. The forward-looking vision of geostructures thermal activation  
653 represents in this scenario a new and crucial element that the geotechnical culture provides to the community.

654

## 655 **ACKNOWLEDGEMENTS**

656 The Authors wish to thank all the people, organizations and institutions who have contributed in different ways  
657 and phases of the research: students and colleagues of the Politecnico di Torino, professionals and  
658 administrators of the companies involved in the projects of the line 1 and line 2 of Turin metro.

659 Financial support to the research has been granted by the project 'Enertun' funded by the Polo Regionale di  
660 Innovazione ENERMHY, the Proof of Concept project funded by Fondazione San Paolo, the COST Action  
661 TU 1405 GABI and research contracts by Systra SA and Iren SpA.

662 Data used are available from the corresponding author by request.

663

664 **REFERENCES**

- 665 Adam, D., Markiewicz, R. 2009. Energy from earth-coupled structures, foundations, tunnels and sewers, *Geotechnique*  
666 59: 229-236, doi.org/10.1680/geot.2009.59.3.229.
- 667 Alvi, M.R., Insana, A., Barla, M. (2022). Thermal performance assessment of an energy lining for the Lyon-Turin base  
668 tunnel. *Soils and Rocks* 45 (1):e2022000722.
- 669 Amis, T., Robinson, C.A.W., Wong, S., 2010. Integrating Geothermal Loops into the Diaphragm Walls of the  
670 Knightsbridge Palace Hotel Project. Proceeding 11<sup>th</sup> DFI / EFFC Int. Conf. London 10.
- 671 ASTM 2012. Standard Practice for Using a Guarded-Hot-Plate Apparatus or Thin-Heater Apparatus in the Single-Sided  
672 Mode. ASTM C1044-12. ASTM International, West Conshohocken, PA.
- 673 ASTM 2014. Standard Test Method for Determination of Thermal Conductivity of Soil and Soft Rock by Thermal Needle  
674 Probe Procedure. ASTM D5334-14. ASTM International, West Conshohocken, PA.
- 675 Baralis, M., Barla, M., Bogusz, W., Di Donna, A., Ryzynski, G., Zerun, M. 2018. Geothermal potential of the NE  
676 extension Warsaw metro tunnels, *Environ. Geotech.*: 1-13, doi.org/10.1680/jenge.18.00042.
- 677 Baralis, M., Insana, A., Barla, M. 2020. Energy tunnels for deicing of a bridge deck in Alpine region. In M. Barla, A. Di  
678 Donna, D. Sterpi (eds.), *Challenges and innovation in Geomechanics, Proc. of the 16. International Conference*  
679 *of IACMAG 2020, Torino 1-4 Luglio 2020*, Vol. 2.
- 680 Barla, M., Baralis, M., Insana, A., Zacco, F., Aiassa, S., Antolini, F., Azzarone, F., Marchetti, P. 2019a. Feasibility study  
681 for the thermal activation of Turin Metro Line 2. In D. Peila, G. Viggiani, T. Celestino (eds.), *Tunnels and*  
682 *Underground Cities: Engineering and Innovation Meet Archaeology, Architecture and Art- Proceedings of the*  
683 *WTC 2019 ITAAITES World Tunnel Congress*: 231-240. CRC Press/Balkema.
- 684 Barla, M., Baralis, M., Insana, A., Aiassa, S., Antolini, F., Vigna, F., Azzarone, F., Marchetti, P. 2020. On the thermal  
685 activation of Turin metro Line 2 tunnels. In M. Barla, A. Di Donna, D. Sterpi (eds.), *Challenges and innovation*  
686 *in Geomechanics, Proc. of the 16. International Conference of IACMAG 2020, Torino 1-4 Luglio 2020*, Vol. 2.
- 687 Barla, M., Barla, G., 2012. Torino subsoil characterisation by combining site investigations and numerical modelling.  
688 *Geomech. Tunn.* 5: 214-231.
- 689 Barla, G., Barla, M., Bonini, M., Debernardi, D., Perino, A., Antolini, F., Gilardi, M., 2015. 3D thermo-hydro modeling  
690 and real-time monitoring for a geothermal system in Torino, Italy. In: *Proceedings of the XVI ECSMGE*  
691 *Geotechnical Engineering for Infrastructure and Development*: 2481-2486.
- 692 Barla, M., Di Donna, A. 2016. Editorial Themed issue on energy geostructures. *Environ. Geotech.* 3: 188-189.
- 693 Barla M., Di Donna, A. 2018. Energy tunnels: concept and design aspects. *Undergr. Space* 3: 268-276,  
694 doi.org/10.1016/j.undsp.2018.03.003.
- 695 Barla, M., Di Donna, A., Baralis, M. 2018b. City-scale analysis of subsoil thermal conditions due to geothermal  
696 exploitation. *Environ. Geotech.*: 1-11.
- 697 Barla M., Di Donna, A., Insana, A. 2019b. A novel real-scale experimental prototype of energy tunnel. *Tunn. Undergr.*  
698 *Space Technol.* 87: 1-14.
- 699 Barla M., Di Donna A., Perino A. 2016. Application of energy tunnels to an urban environment. *Geothermics* 61: 104-  
700 113, doi.org/10.1016/j.geothermics.2016.01.014.
- 701 Barla, M., Di Donna, A., Santi, A. 2018a. Energy and mechanical aspects on the thermal activation of diaphragm walls  
702 for heating and cooling. *Renewable Energy.* 10.1016/j.renene.2018.10.074

703 Barla M., Perino A. 2014. Energy from geo-structures: a topic of growing interest. *Environ. Geotech.* 2: 3-7,  
704 doi.org/10.1680/envgeo.13.00106.

705 Bidarmaghz, A., Narsilio, G.A. 2018. Heat exchange mechanisms in energy tunnel systems. *Geomech. Energy Environ*  
706 16: 83-95. doi.org/10.1016/j.gete.2018.07.004.

707 Bidarmaghz, A., Narsilio, G.A., Buhmann, P., Moormann, C., Westrich, B. 2017. Thermal interaction between tunnel  
708 ground heat exchangers and borehole heat exchangers, *Geomech. Energy Environ.* 10: 29-41,  
709 doi.org/10.1016/j.gete.2017.05.001.

710 Bidarmaghz et al. 2023. Investigating the effectiveness of energy tunnels in cooling underground substations. In M. Barla,  
711 A. Di Donna, D. Sterpi (eds.), *Challenges and innovation in Geomechanics, Proc. of the 16. International*  
712 *Conference of IACMAG 2020, Torino 1-4 Luglio 2020*, Vol. 2.

713 Bottino G., Civita M.V. 1986. Engineering geological features and mapping of subsurface in the metropolitan area of  
714 Turin, North Italy. In: *5. International IAEG Congress. Buenos Aires: 1741-1753.*

715 Bouazza, A., Adam, D., Rao Singh, M., Ranjith, P.G. 2011. Direct geothermal energy from geostructures. In: *Aust.*  
716 *Geotherm. Energy Conf. 2011: 21-24.*

717 Bourne-Webb, P., da Costa Gonçalves, R. 2016. On the exploitation of ground heat using transportation infrastructure.  
718 *Procedia Engineering: 1333-1340*, doi.org/10.1016/j.proeng.2016.06.157.

719 Bourne-Webb, P., Bodas Freitas, T.M., da Costa Gonçalves, R.A. 2016. Thermal and mechanical aspects of the response  
720 of embedded retaining walls used as shallow geothermal heat exchangers. *Energy Build.* 125: 130-141,  
721 doi.org/10.1016/j.enbuild.2016.04.075.

722 Brandl H. 2006. Energy foundations and other thermo-active ground structures. *Géotechnique* 56: 81-122.

723 Buhmann, P., Moormann, C., Westrich, B., Pralle, N., Friedemann, W. (2016). Tunnel geothermics—A German  
724 experience with renewable energy concepts in tunnel projects. *Geomechanics for Energy and the Environment*  
725 8, 1-7.

726 CFMS/SYNTTEC INGENIERIE/SOFFONS-FNTP (2016). Recommandations pour la conception, le dimensionnement et  
727 la mise en oeuvre des géostructures thermiques. *Rev. Fr. Geotech.* 149(1), 1-120.

728 Connolly D. 2017. Heat Roadmap Europe: Quantitative comparison between the electricity, heating, and cooling sectors  
729 for different European countries. *Energy*, doi.org/10.1016/j.energy.2017.07.037.

730 Cousin, B., Rotta, A.F., Bourget, A., Rognon, F., Laloui L. 2019. Energy performance and economic feasibility of energy  
731 segmental linings for subway tunnels. *Tunn. Undergr. Space Technol.* 91, 102997,  
732 doi.org/10.1016/j.tust.2019.102997.

733 Delerablee, Y. (2019). Intégration thermique et mécanique des géostructures thermiques: de l'échelle du bâtiment à  
734 l'échelle de la cité. PhD thesis, Université Paris-Est. In French.

735 Di Donna A., Barla M. 2016. The role of ground conditions and properties on the efficiency of energy tunnels. *Environ.*  
736 *Geotech.* 3, doi.org/10.1680/jenge.15.00030.

737 Di Donna, A., Cecinato, F., Loveridge, F., Barla, M. 2016. Energy performance of diaphragm walls used as heat  
738 exchangers. *Proc. Inst. Civ. Eng. Geotech. Eng.:* 1-14, doi.org/10.1680/jgeen.

739 Di Donna, A., Barla, M., Amis, T. 2017. Energy geostructures: a collection of data from real applications. *15. IACMAG,*  
740 *19-23 ottobre, Wuhan, China.*

741 Diersch H.J.G. 2009. DHI Wasy Software - Feflow 6.1 – Finite Element Subsurface Flow & Transport Simulation System:  
742 Reference Manual.

743 Directive 2009/28/EC. Directive 2009/28/EC of the European parliament and of the council of 23/4/2009, *Off. J. Eur.*  
744 *Union* 140: 16-62, doi.org/10.3000/17252555.L\_2009.140.eng.

745 Dornberger S.C., Rotta Loria, A.F., Zhang, M., Bu, L., Epard, J.L., Turberg, P., 2020. Heat exchange potential of energy  
746 tunnels for different internal airflow characteristics. *Geomechanics for Energy and the Environment*, 100229,  
747 ISSN 2352-3808, https://doi.org/10.1016/j.gete.2020.100229.

748 Epting, J., Baralis, M., Künze, R., Mueller, M.H., Insana, A., Barla, M., Huggenberger, P., 2020. Geothermal potential of  
749 tunnel infrastructures - development of tools at the city-scale of Basel, Switzerland. *Geothermics* 83, 101734.

750 European Commission 2016. Overview of support activities and projects of the European Union on energy efficiency and  
751 renewable energy in the heating & cooling sector. Publications Office of the European Union, Luxembourg,  
752 doi.org/10.2826/607102.

753 European Heat Pump Association 2019. European Heat Pump Market and Statistics - Report 2019.

754 Franzius J.N., Pralle N. 2011. Turning segmental tunnels into sources of renewable energy. *Proc. ICE - Civ. Eng.* 164:  
755 35-40.

756 Frodl S., Franzius J.N., Bartl T. 2010. Design and construction of the tunnel geothermal system in Jenbach / Planung und  
757 Bau der Tunnel-Geothermieanlage in Jenbach. *Geomech. Tunn.* 3: 658-668, doi.org/10.1002/geot.201000037.

758 GSHPA, 2012. Thermal pile design, installation and materials standards. Issue 1.0, Ground Source Heat Pump  
759 Association, Milton Keynes, UK.

760 Insana, A., Barla, M. 2020. Experimental and numerical investigations on the energy performance of a thermo-active  
761 tunnel. *Renewable Energy*. 10.1016/j.renene.2020.01.086

762 Insana, A., Barla, M., Sulem, J. 2020. Energy tunnel linings thermo-mechanical performance: comparison between field  
763 observations and numerical modelling. *Int. Conf. on Energy Geotechnics, La Jolla, California, USA - September*  
764 *20-23, 2020*.

765 Insana, 2020. Thermal and structural performance of energy tunnels. PhD thesis, Politecnico di Torino, 436 pp.

766 Islam, S., Fukuhara, T., Watanabe, H., Nakamura, A. (2006). Horizontal U-Tube road heating system using tunnel ground  
767 heat. *Journal of Snow Engineering of Japan* 22(3), 229-234.

768 Itasca 2016. Flac ver.7.0 User's manual.

769 Laloui L., Di Donna A. 2013. *Energy geostructures: innovation in underground engineering*. ISTE Ltd and John Wiley  
770 & Sons Inc.

771 Lee C., Park S., Won J., Jeoung J., Sohn B., Choi H. 2012. Evaluation of thermal performance of energy textile installed  
772 in Tunnel. *Renew. Energy* 42: 11-22.

773 Lee, C., Park, S., Choi, H.-J., Lee, I.-M., Choi, H. (2016). Development of energy textile to use geothermal energy in  
774 tunnels. *Tunnelling and Underground Space Technology*, 59, 105-113.

775 Loveridge, F., Low, J., Powrie, W. 2017. Site investigation for energy geostructures. *Quarterly Journal of Engineering*  
776 *Geology and Hydrogeology* 50: 158-168, doi.org/10.1144/qjegh2016-027.

777 Lund, J.W., Freeston, D.H., Boyd, T.L. 2011. Direct utilization of geothermal energy 2010 worldwide review.  
778 *Geothermics* 40: 159-180, doi.org/10.1016/j.geothermics.2015.11.004.

779 Ma, C., Di Donna, A., Dias, D., Zhang, J. (2021). Numerical investigations of the tunnel environment effect on the  
780 performance of energy tunnels. *Renewable Energy* 172, 1279-1292.

781 Ma, C., Di Donna, A., Dias, D. (2022). Numerical study on the thermos-hydro-mechanical behaviour of an energy tunnel  
782 in a coarse soil. *Computers and Geotechnics* 151, 105003.

783 Makasis, N., Narsilio, G.A. (2020). Energy diaphragm wall thermal design: The effects of pipe configuration and spacing.  
784 *Renewable Energy* 154, 476–487.

785 Makasis, N., Narsilio, G.A. (2020). A case study on the application of energy tunnels in Sydney, Australia. In M. Barla,  
786 A. Di Donna, D. Sterpi (eds.), *Challenges and innovation in Geomechanics, Proc. of the 16. International*  
787 *Conference of IACMAG 2020, Torino 1-4 Luglio 2020*, Vol. 2.

788 Meibodi, S.S., Loveridge, F. 2022. The future role of energy geostructures in fifth generation district heating and cooling  
789 networks, *Energy* 240, 2022, 122481, ISSN 0360-5442, <https://doi.org/10.1016/j.energy.2021.122481>.

790 Moormann, C, Buhmann, P., Westrich, B. (2018). Web-based application for the investigation of thermally activated  
791 tunnels. *Tunnel* 6, 46-56.

792 Moormann C., Buhmann P., Friedemann W., Homuth S., Pralle N. 2016. Tunnel geothermics - International experience  
793 with renewable energy concepts in tunnelling / Tunnelgeothermie - Internationale Erfahrungen zu regenerativen  
794 Energiekonzepten im Tunnelbau. *Geomech. Tunn.* 9: 467-480.

795 Nicholson, D.P., Chen, Q., de Silva, M., Winter, A., Winterling, R. 2014. The design of thermal tunnel energy segments  
796 for Crossrail, UK. *Eng. Sustain.* 167: 118-134.

797 Ogunleye, O., Singh, R.M., Cecinato, F., Chan Choi, J. 2020. Effect of intermittent operation on the thermal efficiency  
798 of energy tunnels under varying tunnel air temperature. *Renew. Energy* 146: 2646-2658,  
799 [doi.org/10.1016/j.renene.2019.08.088](https://doi.org/10.1016/j.renene.2019.08.088).

800 Peltier, M., Rotta Loria, A.F., Lepage, L., Garin, E., Laloui, L. (2019). Numerical investigation of the convection heat  
801 transfer driven by airflows in underground tunnels. *Applied Thermal Engineering* 159, 113844.

802 Preene M., W. Powrie, 2009. Ground energy systems: from analysis to geotechnical design. *Geotechnique* 59: 261-271,  
803 [doi.org/10.1680/geot.2009.59.3.261](https://doi.org/10.1680/geot.2009.59.3.261).

804 Ronchi, F., Salciarini, D., Cavalagli, N., Tamagnini, C. 2018. Thermal response prediction of a prototype Energy Micro-  
805 Pile. *Geomechanics for Energy and the Environment* 16, December 2018: 64-82,  
806 [doi.org/10.1016/j.gete.2018.07.001](https://doi.org/10.1016/j.gete.2018.07.001).

807 Rosso E., Insana A., Vesipa R., Barla M. 2021. Optimization of the hydraulic circuit for energy tunnels. *EURO:TUN*  
808 *2021, 5<sup>th</sup> International Conference on Computational Methods and Information Models in Tunneling*, Ruhr  
809 University Bochum, 27-29 October 2021. Under review.

810 Rotta Loria, A.F., Di Donna, A., Zhang, M. (2022). Stresses and deformations induced by geothermal operations of energy  
811 tunnels. *Tunnelling and Underground Space Technology* 124, 104438.

812 Rybach, L. (1995). Thermal waters in deep Alpine tunnels. *Geothermics* 24(5–6), 631-637.

813 Schneider M., Moormann C. 2010. GeoTU6 – a geothermal Research Project for Tunnels. *Tunnel* 2: 14-21.

814 SIA (2005). Utilisation de la chaleur du sol par des ouvrages de fondation et de soutènement en béton, guide pour la  
815 conception, la réalisation et la maintenance. Swiss Society of Engineers and Architects, Geneva, Switzerland.

816 Sterpi, D., Angelotti, A., Corti, D., Ramus, M. 2014. Numerical analysis of heat transfer in thermo-active diaphragm  
817 walls. *Numer. Methods Geotech. Eng.:* 1043–1048.

818 Sterpi, D., Angelotti, A., Habibzadeh-Bigdarvish, O., Jalili, D. (2018). Assessment of thermal behaviour of thermoactive  
819 diaphragm walls based on monitoring data. *Journal of Rock Mechanics and Geotechnical Engineering* 10, 1145-  
820 1153.

821 Tinti, F., Boldini, D., Ferrari, M., Lanconelli, M., Kasmae, S., Bruno, R., Egger, H., Voza, A., Zurlo, R. 2017.  
822 Exploitation of geothermal energy using tunnel lining technology in a mountain environment. A feasibility study

823 for the Brenner Base tunnel – BBT. *Tunnelling and Und. Space Tech.* 70:182-203,  
824 doi.org/10.1016/j.tust.2017.07.011.

825 Unterberger, W., Hofinger, H, Grünstäudl, T. Adam, D., Markiewicz, R. (2004). Utilization of Tunnels as Source of  
826 Ground Heat and Cooling – \_Practical Applications in Austria. In: Proceedings of the ISRM International  
827 Symposium 3rd ARMS, Kyoto, 2004, 421–426.

828 Vieira, A., Alberdi-Pagola, M., Christodoulides, P., Javed, S., Loveridge, P., Nguyen, F., Cecinato F. et al. 2017.  
829 Characterisation of ground thermal and thermo-mechanical behaviour for shallow geothermal energy  
830 applications. *Energies MDPI* 10(12).

831 Vieira, A., Alberdi-Pagola, M., Barla, M., Christodoulides, P., Florides, G., Insana, A., Javed, S., Maranha, J., Milenic,  
832 D., Prodan, I., Salciarini, D. (2022). Site characterization for the design of thermoactive geostructures. *Soils and  
833 Rocks* 45(1):e2022001022.

834 Wilhelm J., Rybach L. 2003. The geothermal potential of Swiss Alpine tunnels. *Geothermics* 32: 557-568.

835 Zannin, J., Ferrari, A., Larrey-Lassalle, P., Laloui, L. (2020). Early-stage thermal performance design of thermo-active  
836 walls implemented in underground energy infrastructures. *Geomechanics for Energy and the Environment*.

837 Zhang G., Xia C., Sun M., Zou Y., Xiao S. 2013. A new model and analytical solution for the heat conduction of tunnel  
838 lining ground heat exchangers. *Cold Reg. Sci. Technol.* 88: 59-66.

839 Zhang, G., Xia, C., Yang, Y., Sun, M., Zou, Y. 2014. Experimental study on the thermal performance of tunnel lining  
840 ground heat exchangers. *Energy Build.* 77: 149-157, doi.org/10.1016/j.enbuild.2014.03.043.

841 Zhang, G., Guo, Y., Zhou, Y., Ye, M., Chen, R., Zhang, H., Yang, J., Chen, J., Zhang, M., Lian, Y., Liu, C. 2016.  
842 Experimental study on the thermal performance of tunnel lining GHE under groundwater flow. *Appl. Therm.  
843 Eng.* 106: 784-795, doi.org/10.1016/j.applthermaleng.2016.06.041.